DMD Fast Forward. Published on March 20, 2008 as doi:10.1124/dmd.107.019182

Predictive Physiologically-Based Pharmacokinetic (PBPK) Model for Antibody-Directed Enzyme Prodrug Therapy (ADEPT)

Lanyan Fang[1] and Duxin Sun*

Division of Pharmaceutics, College of Pharmacy, The Ohio State University, Columbus, OH 43210

DMD Fast Forward. Published on March 20, 2008 as DOI: 10.1124/dmd.107.019182
This article has not been copyedited and formatted. The final version may differ from this version.

Running title: Predictive PBPK for ADEPT

Corresponding author:

Duxin Sun, Ph.D. Division of Pharmaceutics, College of Pharmacy, The Ohio State University, 500 W 12th Ave, Columbus, OH 43210. Tel: 614-292-4381; Fax: 614-292-7766; email: sun.176@osu.edu

Number of text page: 20

Number of figure: 8

Number of table: 1

Number of reference: 28

Number of words in abstract: 249

Number of words in introduction: 958

Number of words in discussion: 1199

Abbreviations: PBPK: Physiologically based pharmacokinetic model; GA: Geldanamycin; FcRn: Neonatal Fc-receptor; ADEPT: Antibody-directed enzyme prodrug therapy; AbE: Antibody-enzyme conjugates; TAG-72: Tumor associated glycoprotein 72; P_A: Effective permeability coefficients; AUC: Area under the curve

DMD Fast Forward. Published on March 20, 2008 as DOI: 10.1124/dmd.107.019182
This article has not been copyedited and formatted. The final version may differ from this version.

Abstract

Antibody-directed enzyme prodrug therapy (ADEPT) using anti-TAG-72 antibody and Geldanamycin (GA) prodrug was validated *in vitro*. To understand the complexity and to explore optimal therapeutic regimens for ADEPT *in vivo*, a physiologically-based pharmacokinetic model (PBPK) is applied to analyze each anatomical component/organ. The baseline model predicts that active drug tumor/plasma exposure (AUC) ratio is 2-fold although antibody-enzyme conjugates (AbE) are distributed into tumor up to 9-fold higher than in plasma. However, the active drug tumor/plasma AUC ratio can be increased up to 100-fold when AbE are depleted from plasma. Similarly, the active drug tumor/plasma AUC ratio can be increased from 2- to 6-fold when the intrinsic clearance of AbE is accelerated by 10-fold. Several sensitive parameters are identified: 1) increasing flow inside tumor ($J_{iso,tumor}$) significantly increases active drug tumor/plasma AUC ratio; 2) increasing permeability of prodrug (from range $1.4X10^{-6}$ to $1.4X10^{-4}$ cm/s) increases active drug tumor/plasma AUC ratio significantly, while active drug permeability enhancement (from range $5X10^{-4}$ to $5X10^{-2}$ cm/s) has minimal effect; 3) decreasing Emax and increasing EC50 for converting prodrug to active drug increase tumor/plasma AUC ratio for active drug. The PBPK model predicts that the optimal dosing interval between AbE and prodrug administration is five days, the optimal AbE dose is 0.1 Bmax, and the optimal dose for GA prodrug is 60 mg/kg. The current PBPK model successfully identifies sensitive parameters and predicts optimal dosing regimen for ADEPT.

DMD Fast Forward. Published on March 20, 2008 as DOI: 10.1124/dmd.107.019182
This article has not been copyedited and formatted. The final version may differ from this version.

Introduction

ADEPT was proposed by Dr. Bagshawe over two decades ago (Bagshawe, 1987; Bagshawe et al., 1988). ADEPT is a two step process: in the first step, a drug-activating enzyme is targeted to the tumors by a tumor targeting antibody (via AbE); in the second step, a nontoxic prodrug is administered systemically and converted to the active drug with high tumor concentration by the localized enzyme. However, the prodrug remains inactive in normal tissues (without drug-activating enzyme) and thus decreases its nonspecific toxicity. ADEPT provides many advantages (Bagshawe et al., 1999): (A) Amplification: each localized AbE molecule converts a larger number of nontoxic prodrugs to potent active drugs and increases the tumor active drug concentration. (B) By-stander effect: the locally activated drug molecules with high lipophilicity can diffuse into the cancer cells regardless the heterogeneous antigen expression. The by-stander effect addresses the issues of poor tumor penetration of AbE. (C) AbE do not need to be internalized into each cancer cell for prodrug activation.

This is a rather complex therapeutic regimen considering the following facts (Xu and McLeod, 2001): (A) At least two components or steps are indicated in ADEPT, i.e., AbE should be specifically delivered to the desired tumor site and the nontoxic prodrug should be activated in the target site by the pre-delivered enzyme. Increasing therapeutic steps always makes it harder to control and predict the outcome, so better understanding of the therapy itself and optimal design are necessary. (B) High expression level of antigen in tumors but low level in normal tissues is required for AbE tumor targeting. (C) AbE might not penetrate into the target tissues. (D) Elimination of the biological molecules (AbE) might be nonlinear. (E) The prodrug needs to be enzyme-specifically activated and minimal nonspecific

activation. Large difference of cytotoxicity and other properties between the prodrug and activated drug is desired, such as low permeability to the cell membrane is preferred for the prodrug while the high permeability is preferred for the activated drug (Syrigos and Epenetos, 1999).

Due to the complexity of ADEPT, it would be ideal to predict the therapeutic outcome before the large-scale lengthy and costly preclinical and clinical studies are undertaken. Application of pharmacokinetics (PK) and pharmacodynamics (PD) studies has been shown to guide and expedite drug development (Galluppi et al., 2001). The urgency of PK/PD modeling is clearly demonstrated in U.S. Food and Drug Administration (FDA) guidance (FDA, 1999). It is without question that using mathematical modeling and decomposing the complex system into elementary components will help understand the complex ADEPT and optimize the therapeutic regimen. Few publications have been published using mathematical modeling method to provide insights and guides for ADEPT therapy (Yuan et al., 1991; Baxter and Jain, 1996; Varner, 2005). However, these studies assumed simple compartment model for AbE, prodrug and active drug. Although informative, compartment model is very limited to describe the pharmacokinetic properties of biological molecules. PBPK has been proposed to predict the pharmacokinetics of antibodies itself (Baxter et al., 1994; Baxter et al., 1995; Friedrich et al., 2002; Ferl et al., 2005). PBPK approach is more physiologically relevant and allows for integration of all anatomical compartments together as they are in the biological system. This will enable the accurate predication of the system change with each compartment variation. The current study intend to apply PBPK modeling to simulate and predict the outcome of ADEPT. PBPK modeling will be able to incorporate special features of ADEPT components, such as convection is more likely to contribute to the AbE

distribution process; FcRn is important for antibody recycling and elimination; and the tumor size might change significantly during the ADEPT course.

In our previous study, we have utilized anti-TAG-72 (tumor associated glycoprotein 72) antibody (HuCC49ΔCH2) to deliver a drug activating enzyme for GA prodrug activation in ADEPT (Cheng et al., 2005; Fang et al., 2006). It was shown that HuCC49ΔCH2-β-galactosidase conjugates were highly specific and enzymatically active. The conjugates were demonstrated to activate the GA prodrug and reduce the IC50 of prodrug to 1μM from 25μM against LS174T, colorectal cancer cells with high levels of TAG-72 expression. Several important factors contribute to the advantages of using the anti-TAG-72 antibody and GA prodrug: (A) The TAG-72 antigen is primarily expressed in tumors with almost no detectable expression in normal tissues. (B) The humanized anti-TAG-72 antibody (HuCC49ΔCH2) was used for tumor detection in human clinical trials and shown no immunological response. (C) HuCC49ΔCH2 was shown to localize in the extracellular matrix. The large amount of antigen in the extracellular space may trap a large amount of AbE (Knox R J, 1999). Unlike other antibodies against tumor cell membrane antigen, HuCC49ΔCH2 may avoid the problem of internalization of AbE for lysosomal degradation. (D) The GA prodrug with a sugar moiety is more polar and less membrane permeable than the activated drug with high lipophilicity (Tietze et al., 2002).

The current study aims to use the PBPK approach to understand the complexity of ADEPT therapy and to guide AbE selection, AbE dose regimen (dose and dosing interval before prodrug administration), prodrug design and prodrug dose. The objectives are the following: (A) To build three levels of PBPK model for AbE, prodrug and active drug and to provide a quantitative basis to carry out ADEPT therapy *in vivo*. (B) To identify the sensitive

factors or parameters controlling the ADEPT process including antigen expression in tumor tissues, antibody affinity to antigen, clearance and depletion of AbE, prodrug and active drug permeability. (C) Dosing regimen optimization for AbE and prodrug administration to achieve maximal active drug concentration in tumors and minimal active drug in blood and normal tissues.

Methods

Model Development

This model was built based on the LS174T colorectal cancer cell xenograft mouse model. The model was developed to study the distribution and targeting of AbE, and the activation of prodrug to active drug based on previously published models (Baxter et al., 1994; Baxter et al., 1995; Ferl et al., 2005). A whole-body physiologically based model is used in which the major organs of the mice are represented as compartments. Each compartment is connected in an anatomical manner by the systemic and lymphatic circulation (Figure 1). The organ compartments are then further subdivided into vascular and extravascular subcompartments.

The detailed PBPK description of AbE is adapted from a previous model for antibody against colorectal tumor antigen (Ferl et al., 2005). Since effective AbE do not affect antigen-antibody binding process and AbE have similar molecular size range as antibody, it is hypothesized that AbE distribute into tissues under the same driving forces as antibody alone. The main transport processes in the AbE include: (A) AbE transport across capillary walls through convection and diffusion; (B) AbE reversibly and specifically bind to tumor antigens with saturation. (C) AbE are eliminated through the liver; (D) In skin and muscle, FcRn

unbound AbE undergo endosomal degradation, while FcRn bound AbE are protected and recycled back to vascular circulation. FcRn sites can be extended to other organs where FcRn receptors are expressed in the model. In the current model, FcRn receptors are added mainly in skin and muscle based on findings by Dr. Ferl et. al. that a good fitting between experimental data and simulated results can be obtained when FcRn sites are considered only in skin and muscle.

The main transport processes for prodrug and active drug model include: (A) Transport of prodrug and active drug is diffusion-limited across the endothelial wall of vascular and extravascular spaces. (B) The metabolism of prodrug and active drug is predominantly through liver. (C) The connection among AbE, prodrug, and active drug is that the predisposed AbE convert prodrug to active drug in each specified organ subcompartment.

The tumor mass was found to be highly variable based on the previous studies, thus a variable tumor mass submodel was adopted to reflect the real tumor physiology (Ferl et al., 2005). This phenomenon was also confirmed in rapid growing LS174T xenograft model based on our own experience. The model nomenclature is given in Appendix A and mathematical equations accounting for the mass balance are presented in Appendix B, respectively.

Model baseline Parameters

All the widely accepted physiological parameters for mice are from previous publications (Baxter et al., 1995; Baxter and Jain, 1996; Ferl et al., 2005). These physiological parameters are summarized in Appendix A. For AbE related parameters, the baseline values of all parameters are obtained or estimated from Dr. Ferl et al.'s results (Ferl et al., 2005).

Considering the values of these constants may vary with different antibodies, selected enzyme and tumor cell lines, we arbitrarily choose baseline values based on literature values and our own experimental results for simulation studies. For prodrug and active drug, most parameters are from the literature and our own experimental data for GA-prodrug (Fang et al., 2006). The effective permeability coefficients (P_A) of prodrug and active drug are assumed to be very different based on the high hydrophilic prodrug moiety and hydrophobic properties for active drug. This assumption is based on the fact that active drug needs to be more permeable than prodrug in order to penetrate into the tumor tissues in ADEPT system. All baseline values used are summarized in Table 1.

Time and dosing schedules of simulation studies

In the sensitivity analysis, the time interval between antibody-enzyme conjugate (AbE) and prodrug is fixed at 3 days based on the following rationale: (A) Antibody alone distributed into tumor tissues at the highest level at 3 days post Antibody injection in the previous publication (Ferl et al., 2005). (B) This fixed interval allows us to study the effect of other sensitive parameters separately (such as antigen expression levels, AbE affinity to antigen, clearance and depletion of AbE, AbE enzymatic activity, prodrug permeability). Both AbE and prodrug are administered as a single bolus dose injection in this simulation.

The baseline dose of a single bolus AbE injection was chosen to be 1/10 of the maximum binding capacity of the tumor tissues (Bmax). This selection was based on the result from a previously study (Yuan et al., 1991). The baseline dose of prodrug injection was chosen to allow the active drug concentration above IC50 in the tumor tissues.

Model simulation and Simulation criteria

Three factors are critical for ADEPT to succeed: (A) active drug tumor/plasma exposure (AUC) ratio, (B) minimum effective active drug tumor AUC, and (C) the absolute tolerable plasma AUC for active drug. As indicated in Varner's study (Varner, 2005), a tumor to plasma ratio of 10 to 1 for active drug concentration or AUC is sufficient for ADEPT efficacy, while the absolute tumor and tolerable plasma exposure will depend on the specific active drug's toxicity and efficacy. In the current study, we set the absolute active drug plasma concentration below IC50 (which is 1μM for activated GA prodrug against colon cancer cells LS174T) in plasma and normal tissues, while tumor active drug concentration above 1μM. The reason of setting IC50 rather than exposure is because IC50 is an easier parameter to get in the early stage of preclinical study when PBPK modeling is actually needed to guide further animal or human study design.

Simulation Software

Berkeley Madonna version 8.3.9 is used in the current simulation study. Rosenbrock (stiff) is the selected integration method.

Results:

AbE, prodrug and active drug distribution with the baseline parameter assumption

We first analyzed the distribution of AbE, prodrug and active drug with the baseline physiological, biological and physical parameters (Figure 2). As indicated in Figure 2A and 2B, the tumor/plasma AbE ratio raises rapidly before day 4 followed by a slowly rising phase

up to day 8. Therefore, the baseline interval between AbE and prodrug injection is selected as 3 days.

The prodrug distribution is rather nonselective between tumor and normal tissues. Prodrug has a much higher concentration in the plasma than in the tumor (Figure 2C). However, the active drug, which is converted from prodrug by the AbE, distributes in the tumor at a higher level than in the plasma. The tumor/plasma concentration or AUC ratio for the active drug is between 1.5 and 2 based on the baseline parameters (Figure 2D).

Depletion of AbE from plasma on day 3 when the prodrug is injected dramatically increased tumor/plasma concentration ratio of the active drug

It was reported previously that tumor/plasma ratio of AbE exceeded 10000:1 in a clinical trial study if a second antibody against AbE conjugate was applied to increase AbE clearance from plasma (Napier et al., 2000). This high ratio of tumor:plasma or tumor:normal tissues for AbE level provided a favorable environment for prodrug activation in tumors in theory.

However, it is not clear how this high tumor:plasma ratio of AbE will affect the active drug concentration in tumors and tumor:plasma ratio. Therefore, we utilized the PBPK model to validate the effect on the active drug concentration in the tumor and plasma by removing AbE from the plasma by a secondary clearing antibody. On day 3 when prodrug is injected into the system, the AbE concentration in the plasma is set to zero to reflect the removal. As shown in Figure 3A, active drug concentration in the plasma is dramatically reduced but not to zero when AbE in the plasma is removed. This is different from the previous study that no conversion of prodrug to active drug was assumed in the plasma and thus the plasma concentration of the active drug is set close to zero (Yuan et al., 1991). Our simulated result

is considered more reasonable since AbE, prodrug and active drug can all be collected back into the circulation from organs such as liver, kidney, lung, and tumor physiologically. Our PBPK model in this study can reflect this phenomenon: the plasma active drug concentration peak time is delayed when AbE is removed indicating that the active drug in other organs can "leak" back into the plasma.

In addition, the active drug concentration in the tumor remains relatively unchanged after AbE is removed from plasma (Figure 3B). This observation could be explained as previous study (Yuan et al., 1991). Prodrug conversion in the plasma will be decreased when AbE is removed from the plasma resulting a higher prodrug concentration systemically; thus, tumor prodrug conversion will be increased because of the high tumor prodrug concentration. The transport from the tumor to other sites may increase due to the concentration difference of active drug, but the accelerated prodrug conversion to active drug compensates this transfer. Thus, the overall net change of the active drug concentration in the tumor is relatively small when AbE is depleted from plasma. Considering the dramatically reduced plasma concentration and almost unchanged tumor concentration, the tumor:plasma concentration ratio is significantly increased for the active drug. The ratio is increased up to 100-fold compared to 2-fold based on the baseline parameters (Figure 3C).

Acceleration of AbE intrinsic clearance significantly increased tumor:plasma AUC ratio of the active drug

Although a second antibody can deplete AbE from the plasma and increase the tumor:plasma ratio of active drug concentration, the second antibody may cause immune response and make ADEPT harder to control. Therefore, another approach is to increase AbE

DMD Fast Forward. Published on March 20, 2008 as DOI: 10.1124/dmd.107.019182
This article has not been copyedited and formatted. The final version may differ from this version.

intrinsic clearance to accelerate removal of AbE from blood circulation (and normal tissues/organs) and reduce residual conjugate activity. We have studied an engineered humanized antibody HuCC49ΔCH2 with clearance of $1.5X10^{-3}$ mL/min (Fang et al., 2007). The high clearance of this humanized antibody was due to the deletion of CH2 domain and glycosylation site.

However, increasing the clearance of AbE might also reduce the uptake and retention of AbE in tumor tissues since the remained AbE inside the body is reduced. Therefore, a delicate balance must be established in order to maximize the absolute tumor retention and tumor/plasma ratio of AbE. PKPB model was utilized to simulate the effect of increasing AbE clearance on active drug concentration in tumors, plasma, and their ratios.

As predicted, increased AbE clearance from circulation leads to reduced AbE concentration (or distribution) in tumor and plasma (Figure 4A and 4B). However, the AUC ratio of active drug in tumor/plasma is significantly increased when intrinsic clearance of AbE is increased from $1.5X10^{-5}$ to $1.5X10^{-3}$ mL/min (Figure 4C). It is worthy noting the nonlinear distribution of AbE in tumor in the PBPK model. AbE distribute into tumor or other tissues in a nonlinear manner because of the capacity-limited binding process. Because of the distribution equilibrium between tumor (or other tissues) and circulation, the nonlinear distribution of AbE in tumor (or other organs) causes nonlinear removal from circulation. Consequently, when intrinsic clearance of AbE is increased from $1.5X10^{-5}$ to $1.5X10^{-4}$ mL/min, AbE concentration in the plasma is reduced to a small extent (Figure 4B). However, when clearance is increased from $1.5X10^{-4}$ to $1.5X10^{-3}$ mL/min, the AbE concentration in the plasma decreased significantly (Figure 4B). Therefore, the nonlinear distribution may have a "buffering" effect when AbE clearance is increased from $1.5X10^{-5}$ to $1.5X10^{-4}$ mL/min,

while this "buffering" effect is saturated when AbE clearance is further increased to $1.5X10^{-3}$ mL/min. Overall, the active drug tumor/plasma AUC ratio increases up to over 6-fold when AbE clearance is increased to $1.5X10^{-3}$ mL/min.

Parameter sensitivity analysis in PBPK modeling of ADEPT

For complex ADEPT therapy, it is beneficial to know the effect of each unknown or estimated parameter on the model for the dose regimen optimization. These parameters include: AbE enzymatic activity, AbE binding affinity to antigen, permeability of prodrug and active drug, and tumor physiological conditions. Since AUC is a more relevant parameter to measure the therapeutic efficacy of active drug in the tumor, tumor/plasma AUC ratio for the active drug was used in the following study.

As shown in the figure 5, a decrease of the enzymatic activity (Emax) of AbE for prodrug conversion rate from baseline 6000 min^{-1} to 600 min^{-1}, the tumor/plasma AUC ratio of active drug increases from 2-fold to 3-fold. Further decrease of Emax has minimal effect (Figure 5A). This is consistent with the previous finding that the prodrug concentrations in both tumor and plasma are constant when Emax is very low, thus the prodrug conversion is limited by the AbE concentration in the individual organ (Yuan et al., 1991). Consequently, initial reduction of Emax leads to increased tumor/plasma AUC ratio; while further reduction of Emax has no effect. However, the effect of EC50 on the tumor/plasma AUC ratio of active drug is opposite to that of Emax. Initial increase of EC50 causes increase of active drug tumor/plasma AUC ratio, while further increase has minimal effect (Figure 5B).

The binding affinity of AbE is determined by on- and off-rate constants. Given the parameters set in table 1, the enhancement of the on-rate constant or reduction of the off-rate

constant does not yield significant active drug tumor/plasma AUC ratio improvement (data not shown). However, the reduction of the on-rate constant or enhancement of the off-rate leads to a decrease of active drug tumor/plasma AUC ratio. This suggests that a medium range on- and off-rate constant of AbE is preferred. Outside this sensitive range of on- or off-rate constants, AbE binding to the antigen has little effect and other factors may dominate (Green et al., 2001). In details, there are two plateaus (i.e., lower affinity and higher affinity) where on- and off- rate have little effect. The parameters in table 1, which are the actual affinity characteristics of the IgG antibody, set the model into the higher affinity plateau end.

To best optimize ADEPT, the permeability of active drug should be larger than that of prodrug since it is desired that active drug can penetrate into the tumors in depth. In order to best define the permeability range of the prodrug and active drug, we tested the sensitivity of permeability in this PBPK model.

For the defined prodrug permeability range ($1.4X10^{-6}$ cm/s to $1.4X10^{-4}$ cm/s), increasing the prodrug permeability has a significant effect on the active drug tumor/plasma AUC ratio (Figure 5C and 5D). As predicted, increasing the prodrug's permeability coefficient from $1.4X10^{-6}$ cm/s to $1.4X10^{-4}$ cm/s consistently increases the active drug tumor/plasma AUC ratio, especially in the first 10 minutes. This can be explained that enhancement of the prodrug permeability can increase the penetration of prodrug into the organs and tumor, increase the prodrug concentration in the organs and tumor, thus reduce the prodrug concentration in the plasma. As a consequence, the prodrug conversion is increased in the tumor while is decreased in the plasma. Therefore, a high prodrug permeability should be preferred in the allowed permeability range ($1.4X10^{-6}$ cm/s to $1.4X10^{-4}$ cm/s). However, for the defined active drug permeability range ($5X10^{-4}$ cm/s to $5X10^{-2}$ cm/s), enhancement of the

permeability coefficient beyond $5X10^{-3}$ cm/s has little effect. This may be due to the fact that significantly high permeability of the active drug can increase the "leak" of active drug from tumor to plasma, thus active drug tumor/plasma AUC ratio can not be further enhanced. Therefore, there is no need to increase active drug permeability to beyond $5X10^{-3}$ cm/s.

Tumor physiology may also significantly affect the outcome of ADEPT therapy. Fluid recirculation flow rate between vascular and interstitial compartment of tumor ($J_{iso,\ tumor}$) is a parameter to evaluate pressure inside tumor. When the pressure inside tumor is very high, $J_{iso,\ tumor}$ is very small. On the other hand, when the tumor is reasonably small and the inside pressure is still low, the blood supply to the tumor is fairly large and $J_{iso,\ tumor}$ is much bigger. As seen in Figure 5E, the enhancement of $J_{iso,\ tumor}$ can significantly increase active drug tumor/plasma AUC ratio. This suggests that the PBPK model is valid to predict that smaller tumors have much better therapeutic outcome after ADEPT treatment.

The determination of time interval between AbE and prodrug administration

The PBPK model showed that active drug tumor/plasma AUC ratio increases as a result of increasing the AbE and prodrug dosing interval up to 5 days. When the interval is longer than 5 days, the AUC ratio decreases with increasing interval time (Figure 6). Thus, the most optimal dosing interval of AbE and prodrug is 5 days in the current study. This is to the contrary of the previous finding that increasing the dosing interval between AbE and prodrug administration may increase active drug tumor/plasma concentration ratio consistently (Yuan et al., 1991). It was shown in the previous study that the concentration ratio increased from under 1 (interval =0 day) to above 10 (interval=14 days). The current PBPK model is believed to provide more accurate prediction. In the baseline parameters, the trapping of the

active drug by the tumor cells was not considered (Kp=1). Thus, as discussed previously, the only way to increase the active drug tumor/plasma AUC or concentration ratio is to increase the difference of the prodrug conversion (through AbE) between the tumor and plasma (Yuan et al., 1991). Meanwhile, the absolute tumor AbE concentration is also very critical. The actual tumor AbE concentration can not be too low; otherwise, the effective tumor prodrug conversion is so slow that the advantage is diminished although the tumor/plasma AbE concentration ratio might be high. The best dosing interval should be balanced between the tumor/plasma AbE concentration ratio and the absolute tumor AbE concentration.

As shown, the tumor localized AbE is highest around day 4 (Figure 2A) and the tumor/plasma AbE concentration ratio is continuously increasing beyond day 4 post AbE injection (Figure 2B). Since the absolute concentration of AbE in tumor becomes lower after day 5, it is reasonable to expect that an optimal dosing interval of 5 days between AbE and prodrug is predicted by the current PBPK model.

ADEPT based on the most optimal parameters

The most optimal parameters from the sensitivity analysis replace the baseline values in the developed PBPK model for ADEPT. The combination of increased AbE clearance ($1.5X10^{-3}$ mL/min) and prolonged interval (Tau=5 days) give the highest tumor/plasma AUC ratio of the active drug. Thus the model with these two newly identified parameters is the selected optimal PBPK model of ADEPT system. Although there are other sensible parameters, replacement of them into the optimal system only have minimal effect. As shown in Figure 7A, tumor/plasma AUC ratio for the active drug is increased up to 10-fold in the optimal model compared to 2-fold using the baseline parameters. In addition, the absolute

tumor concentration for the active drug is above the preset IC50 (1μM) and the plasma active drug concentration is below 1μM (Figure 7B).

AbE and prodrug dose selection based on the optimal PBPK model

The optimal ADEPT should satisfy the following criteria: (A) Tumor/plasma AUC ratio of the active drug is at least 10-fold. (B) Active drug concentration in tumor is higher than 1μM and lower than 1μM in plasma. Therefore, the optimal PBPK model is used to select the optimal doses of AbE and prodrug considering the dosing interval of AbE and prodrug is 5 days.

The model shows that increasing AbE dose from $1X10^{-11}$ mols (0.1Bmax) to $1X10^{-10}$ mols (1Bmax) reduces the tumor/plasma AUC ratio of active drug and increases both tumor and plasma active drug concentrations above 1μM. On the other hand, reducing AbE dose from $1X10^{-11}$ mols (0.1Bmax) to $1X10^{-12}$ mols (0.01Bmax) increases the tumor/plasma AUC ratio, but tumor active drug concentration is below 1μM. Since 1μM is the required concentration for active drug to achieve efficacy against cancer cells, the optimal dose for AbE is $1X10^{-11}$ mols (0.1Bmax) (Figure 8A, 8B and 8C).

Changing prodrug dose has little effect on the tumor/plasma AUC ratio of active drug. The optimal dose of 60mg/kg is selected since it can maintain tumor active drug concentration above 1μM and plasma active drug concentration below 1μM (Figure 8D, 8E and 8F).

Discussion:

Irrespective of the expected complexity, ADEPT therapy has been widely tested by many research groups. Previous studies established systemic approaches to screen effective ADEPT therapeutic regimen from *in vitro* to *in vivo* and further to human clinical trials. In the early clinical trials from 1997-2000, limited colorectal cancer patients were enrolled in the study (Martin et al., 1997; Napier et al., 2000). A5B7 F(ab')$_2$ antibody (against carcinoembryonic antigen, CEA) conjugated to carboxypeptidase G2 (CPG2) was used in the clinical study. To accelerate the clearance of AbE from blood circulation, a clearing antibody SB43-gal (against the active site of CPG2) was applied. The high tumor:plasma ratio of AbE (exceeding 10000:1) provided an advantage for prodrug administration around 50 hours. Benzoic acid mustard-glutamate, which can be converted to the alkylating agent, was the selected prodrug. However, although there was evidence of tumor response by the active drug, the dosing-limiting myelosuppression was observed for the majority of the patients. This myelosuppression was attributed to the presence of active drug in the plasma since prodrug itself wasn't shown to cause toxicity in their previous study. It was suggested that active drug in the circulation was the result of "leakback" from tumor given that no active enzyme was found in plasma.

In 2002, a new phase I clinical trial using a new prodrug and galactosylated AbE was undertaken (Francis et al., 2002). The galactosylated AbE was expected to be cleared faster from circulation without the help of a second clearing antibody. The elegantly designed prodrug was converted to highly potent active drug with a short half life, which was expected to prevent the "leakback" of active drug to the circulation observed in the previous clinical trial. The result of this clinical trial was rather unexpected. Inadequate tumor localization of AbE (median tumor:normal tissue ratios are less than 1) was observed. Therefore, selective

prodrug conversion in the tumor tissue was not observed for almost all the patients except one. The study concluded that each component (or step) of ADEPT must be strictly monitored in order to achieve the optimal therapeutic outcome. AbE with more efficient tumor localization and less immunogenicity was suggested if second clearing antibody was not used.

One critical study was published in 2005 (Sharma et al., 2005). In this study, a recombinant genetic fusion protein, composed of a single-chain Fv antibody and an enzyme, was expressed in *Pichia pastoris* and a glycosylated protein with branched mannose was resulted. The study successfully confirmed the hypothesis in two morphologically different human colon carcinoma xenografts (LS174T and SW1222) that mannosylated fusion protein's clearance from the circulation was accelerated (rapid clearance from plasma within 6 hours), via mannose receptors, without inducing toxicity. Also, the high AbE tumor to plasma ratios of 1400:1 and 339:1 were observed for LS174T and SW1222 models, respectively. In 2006, the clinical trial study result was published (Mayer et al., 2006). Eighty-fold dose escalation from the starting dose of prodrug was carried out and the therapeutic benefit was evaluated.

Although ADEPT was demonstrated to have great potential, improvement on the optimal conditions for better outcome is necessary. From the long development journey, it was suggested that efficient approach to expedite the development process was desired. The use of large molecular proteins (such as AbE) introduces much more complexity to predict the outcome of ADEPT. The PK/PD properties of therapeutic proteins, such as monoclonal antibodies, are far more complicated than small molecular weight therapeutic agents. In details, the absorption is very variable, thus most antibodies on the market are administered

intravenously and subcutaneously; the distribution is often mediated by convection and receptor-mediated transport; there is capacity-limited binding between antigen and antibody; and the elimination is usually expected to be nonlinear. Due to the expected complexity, the best approach to predict PK properties of biological therapeutic agents is PBPK. Many advantages are provided by PBPK modeling: (A) PBPK modeling allows integration of many physiological, physical and biological parameters and translation of them into the *in vivo* therapeutic efficacy prediction. (B) PBPK modeling estimates the tissue-specific concentrations changes as the function of time. (C) PBPK modeling predicts the kinetic changes by variations of physiological parameters. (D) thus PBPK modeling enables the dose regimen scale-up from animal models to future clinical trials (Zhu et al., 1997).

In our current study, we successfully constructed PBPK simulation models for AbE, prodrug and active drug. All these three molecules' pharmacokinetics was interconnected through prodrug activation to active drug by the pretargeted AbE. We conceive this PBPK model is advantageous compared to the previously published compartmental model in the following aspects: (A) The current PBPK model is more physiologically relevant. Our PBPK model integrate all the tissues/organs into the system as they are in the biological body. Thus they reflect the real biological system much better than the compartmental model. For example, the previous compartmental model does not consider the flow collection back from normal organs into the circulation, while this is captured in the current PBPK model (Yuan et al., 1991). Indeed, this phenomenon is confirmed by the previously published clinical trial study, the "leak" back of active drug from regular organs or tumor to the circulation was the main reason for the observed toxicity (Napier et al., 2000). If PBPK model was introduced before this clinical study, the "leak" back issue would be captured and understood better. (B)

PBPK model captures and predicts individual organs/tissue concentration-time response based on each organ's characteristics. For example, the skin and muscle are unique compared to other organs in the current study since FcRn binding sites were found to be in these organs. It will be difficult for previous compartmental model to incorporate those unique features. Thus the current PBPK model is much more flexible in this aspect.

It is also important to note that further refinement of the current PBPK model is necessary. For example, active drug trapping in the tissues is not considered; however, it is more likely that the active drug can be trapped in the tumor cells. It was previously reported that the active metabolite of 17-AG was trapped in the tumor more than the parent compound 17-AAG itself (Xu et al., 2003). Then it is reasonable to expect that active drug would behave similarly since active drug may bind to its target inside the tumor cells. Consequently, the active drug tumor/plasma AUC ratio might be even higher in the real situation. In addition, FcRn binding sites can be extended to other organs in addition to skin and muscle. In the current PBPK model, only skin and muscle are considered to contain FcRn binding sites according to a previous study (Ferl et al., 2005).

In our previous study, we successfully synthesized GA prodrugs suitable for ADEPT therapy (Cheng et al., 2005; Fang et al., 2006). In addition, humanized anti-TAG72 antibody HuCC49ΔCH2 and β-galactosidase were chemically conjugated and tested for specific activation of GA prodrugs. We expect the current PBPK modeling study will shed light on our future ADEPT experiment design and further therapeutic outcome.

Acknowledgements

The authors would like to acknowledge Dr. Nick Holford for his suggestions and kind help in the current study.

Reference

Bagshawe KD (1987) Antibody directed enzymes revive anti-cancer prodrugs concept. *Br J Cancer* **56:**531-532.

Bagshawe KD, Sharma SK, Burke PJ, Melton RG and Knox RJ (1999) Developments with targeted enzymes in cancer therapy. *Curr Opin Immunol* **11:**579-583.

Bagshawe KD, Springer CJ, Searle F, Antoniw P, Sharma SK, Melton RG and Sherwood RF (1988) A cytotoxic agent can be generated selectively at cancer sites. *Br J Cancer* **58:**700-703.

Baxter LT and Jain RK (1996) Pharmacokinetic analysis of the microscopic distribution of enzyme-conjugated antibodies and prodrugs: comparison with experimental data. *Br J Cancer* **73:**447-456.

Baxter LT, Zhu H, Mackensen DG, Butler WF and Jain RK (1995) Biodistribution of monoclonal antibodies: scale-up from mouse to human using a physiologically based pharmacokinetic model. *Cancer Res* **55:**4611-4622.

Baxter LT, Zhu H, Mackensen DG and Jain RK (1994) Physiologically based pharmacokinetic model for specific and nonspecific monoclonal antibodies and fragments in normal tissues and human tumor xenografts in nude mice. *Cancer Res* **54:**1517-1528.

Cheng H, Cao X, Xian M, Fang L, Cai TB, Ji JJ, Tunac JB, Sun D and Wang PG (2005) Synthesis and enzyme-specific activation of carbohydrate-geldanamycin conjugates with potent anticancer activity. *J Med Chem* **48:**645-652.

Fang L, Battisti RF, Cheng H, Reigan P, Xin Y, Shen J, Ross D, Chan KK, Martin EW, Jr., Wang PG and Sun D (2006) Enzyme specific activation of benzoquinone ansamycin prodrugs using HuCC49DeltaCH2-beta-galactosidase conjugates. *J Med Chem* **49:**6290-6297.

Fang L, Holford NH, Hinkle G, Cao X, Xiao JJ, Bloomston M, Gibbs S, Saif OH, Dalton JT, Chan KK, Schlom J, Martin EW, Jr. and Sun D (2007) Population Pharmacokinetics of Humanized Monoclonal Antibody HuCC49{triangleup}CH2 and Murine Antibody CC49 in Colorectal Cancer Patients. *J Clin Pharmacol* **47:**227-237.

FDA (1999) http://www.fda.gov/cber/gdlns/popharm.htm.

Ferl GZ, Wu AM and DiStefano JJ, 3rd (2005) A predictive model of therapeutic monoclonal antibody dynamics and regulation by the neonatal Fc receptor (FcRn). *Ann Biomed Eng* **33:**1640-1652.

Francis RJ, Sharma SK, Springer C, Green AJ, Hope-Stone LD, Sena L, Martin J, Adamson KL, Robbins A, Gumbrell L, O'Malley D, Tsiompanou E, Shahbakhti H, Webley S, Hochhauser D, Hilson AJ, Blakey D and Begent RH (2002) A phase I trial of antibody directed enzyme prodrug therapy (ADEPT) in patients with advanced colorectal carcinoma or other CEA producing tumours. *Br J Cancer* **87:**600-607.

Friedrich SW, Lin SC, Stoll BR, Baxter LT, Munn LL and Jain RK (2002) Antibody-directed effector cell therapy of tumors: analysis and optimization using a physiologically based pharmacokinetic model. *Neoplasia* **4:**449-463.

Galluppi GR, Rogge MC, Roskos LK, Lesko LJ, Green MD, Feigal DW, Jr. and Peck CC (2001) Integration of pharmacokinetic and pharmacodynamic studies in the discovery, development, and review of protein therapeutic agents: a conference report. *Clin Pharmacol Ther* **69:**387-399.

Green AJ, Johnson CJ, Adamson KL and Begent RH (2001) Mathematical model of antibody targeting: important parameters defined using clinical data. *Phys Med Biol* **46:**1679-1693.

Knox R J MR (1999) *Enzyme-prodrug strategies for cancer therapy*. Kluwer Academic / Plenum Publishers.

Martin J, Stribbling SM, Poon GK, Begent RH, Napier M, Sharma SK and Springer CJ (1997) Antibody-directed enzyme prodrug therapy: pharmacokinetics and plasma levels of prodrug and drug in a phase I clinical trial. *Cancer Chemother Pharmacol* **40:**189-201.

Mayer A, Francis RJ, Sharma SK, Tolner B, Springer CJ, Martin J, Boxer GM, Bell J, Green AJ, Hartley JA, Cruickshank C, Wren J, Chester KA and Begent RH (2006) A phase I study of single administration of antibody-directed enzyme prodrug therapy with the recombinant anti-carcinoembryonic antigen antibody-enzyme fusion protein MFECP1 and a bis-iodo phenol mustard prodrug. *Clin Cancer Res* **12:**6509-6516.

Napier MP, Sharma SK, Springer CJ, Bagshawe KD, Green AJ, Martin J, Stribbling SM, Cushen N, O'Malley D and Begent RH (2000) Antibody-directed enzyme prodrug therapy: efficacy and mechanism of action in colorectal carcinoma. *Clin Cancer Res* **6:**765-772.

Rippe B and Haraldsson B (1987) Fluid and protein fluxes across small and large pores in the microvasculature. Application of two-pore equations. *Acta Physiol Scand* **131:**411-428.

Sharma SK, Pedley RB, Bhatia J, Boxer GM, El-Emir E, Qureshi U, Tolner B, Lowe H, Michael NP, Minton N, Begent RH and Chester KA (2005) Sustained tumor regression of human colorectal cancer xenografts using a multifunctional mannosylated fusion protein in antibody-directed enzyme prodrug therapy. *Clin Cancer Res* **11:**814-825.

Syrigos KN and Epenetos AA (1999) Antibody directed enzyme prodrug therapy (ADEPT): a review of the experimental and clinical considerations. *Anticancer Res* **19:**605-613.

Tietze LF, Feuerstein T, Fecher A, Haunert F, Panknin O, Borchers U, Schuberth I and Alves F (2002) Proof of principle in the selective treatment of cancer by antibody-directed enzyme prodrug therapy: the development of a highly potent prodrug. *Angew Chem Int Ed Engl* **41:**759-761.

Varner JD (2005) Systems biology and the mathematical modelling of antibody-directed enzyme prodrug therapy (ADEPT). *Syst Biol (Stevenage)* **152:**291-302.

Xu G and McLeod HL (2001) Strategies for enzyme/prodrug cancer therapy. *Clin Cancer Res* **7:**3314-3324.

Xu L, Eiseman JL, Egorin MJ and D'Argenio DZ (2003) Physiologically-based pharmacokinetics and molecular pharmacodynamics of 17-(allylamino)-17-demethoxygeldanamycin and its active metabolite in tumor-bearing mice. *J Pharmacokinet Pharmacodyn* **30:**185-219.

Yuan F, Baxter LT and Jain RK (1991) Pharmacokinetic analysis of two-step approaches using bifunctional and enzyme-conjugated antibodies. *Cancer Res* **51:**3119-3130.

Zhu H, Baxter LT and Jain RK (1997) Potential and limitations of radioimmunodetection and radioimmunotherapy with monoclonal antibodies. *J Nucl Med* **38:**731-741.

Footnotes

[1]

[1] [1]Current address: Clinical DMPK, Merck & Co., Inc, WP75B-100, 770 Sumneytown Pike, PO Box 4, West Point, PA, 19486[1]

Figure legends:

Figure 1, Basic PBPK structure model for ADEPT therapy in LS174T colorectal caner xenograft model.

Figure 2, Antibody-enzyme conjugate(AbE), prodrug and active drug distribution into tumor and plasma upon baseline parameters. (A) AbE concentration (percentage of injected dose per gram tissue) in the tumor (solid line) and plasma (dotted line); (B) Tumor/plasma AbE concentration ratio; (C) Prodrug concentration in the tumor (solid line) and plasma (dotted line); (D) Tumor/plasma concentration (dotted line) and AUC (solid line) ratio of active drug.

Figure 3, The effect of AbE depletion on the active drug tumor and plasma concentration. (A) Active drug concentration in the plasma when the plasma AbE is removed at day 3 (dotted line) compared to AbE remained in the plasma (solid line). (B) Active drug concentration in the tumor when the plasma AbE is removed at day 3 (dotted line) compared to AbE remained in the plasma (solid line). (C) Active drug concentration in the tumor (solid line) and plasma (dotted line) when the plasma AbE is removed at day 3.

Figure 4, The effect of AbE clearance acceleration on the AbE and active drug distribution in the tumor and plasma. (A) Tumor AbE concentration at different clearance. (B) Plasma AbE concentration at different clearance. (C)Active drug tumor/plasma AUC ratio with changing AbE clearance.

Figure 5, Parameter sensitivity analysis on Emax (A) and EC50 (B) of AbE for prodrug conversion; permeability coefficient of prodrug (C) and active drug (D); and inside tumor flow (D).

Figure 6, Active drug tumor/plasma AUC ratio when prodrug is injected at day 1, 3, 5 and 8 after AbE injection. Time interval of 5 gives the highest tumor/plasma AUC ratio of active drug.

Figure 7, ADEPT based on the most optimal parameters. Active drug tumor/plasma AUC ratio is depicted in Figure A and absolute active drug concentration in the tumor (solid line) and plasma (dotted line) are represented in Figure B.

Figure 8, Dose selection for AbE (A, B and C) and prodrug (D, E, and F).

DMD Fast Forward. Published on March 20, 2008 as DOI: 10.1124/dmd.107.019182
This article has not been copyedited and formatted. The final version may differ from this version.

Table 1, Baseline values of the model of AbE, prodrug, and active drug

Constants	Baseline values	Reference and/or explanations
fup_prodrug	1	Simplify the model
fup_drug	1	
Kp_prodrug	1	Simplify the model
Kp_drug	1	
MW_prodrug (Dalton)	700	Estimation
P_prodrug (cm/s)	$1.4X10^{-5}$	Reference (Yuan et al., 1991), sucrose's P value
P_drug (cm/s)	$5X10^{-3}$	1) 500-fold than prodrug 2) Chosen to be close to lipophilic compounds, such as isopropanol
Emax (1/min)	6000	Estimation
EC50_prodrug (μM)	200	1) Reference (Yuan et al., 1991) 2) Based on our only experiments
Surface Area in muscle (SAmuscle, cm2)	1.24	Estimation
PStumor/PSmuscle	10	Reference (Baxter et al., 1994)
PSliver/PSmuscle	10	Reference (Baxter et al., 1994)
PSorgan/PSmuscle (organs other than liver and tumor)	1	Reference (Baxter et al., 1994)
Clint_prodrug (ml/min)	1	Estimation
Clint_drug (ml/min)	1	Estimation
Dose_AbE (mol)	10^{-11}	0.1 Bmax; based on results from Reference (Yuan et al., 1991)
Interval between AbE and prodrug (days)	3	AbE was shown to distribute into tumor highest around 3 days in Reference (Ferl et al., 2005)

Fig. 1

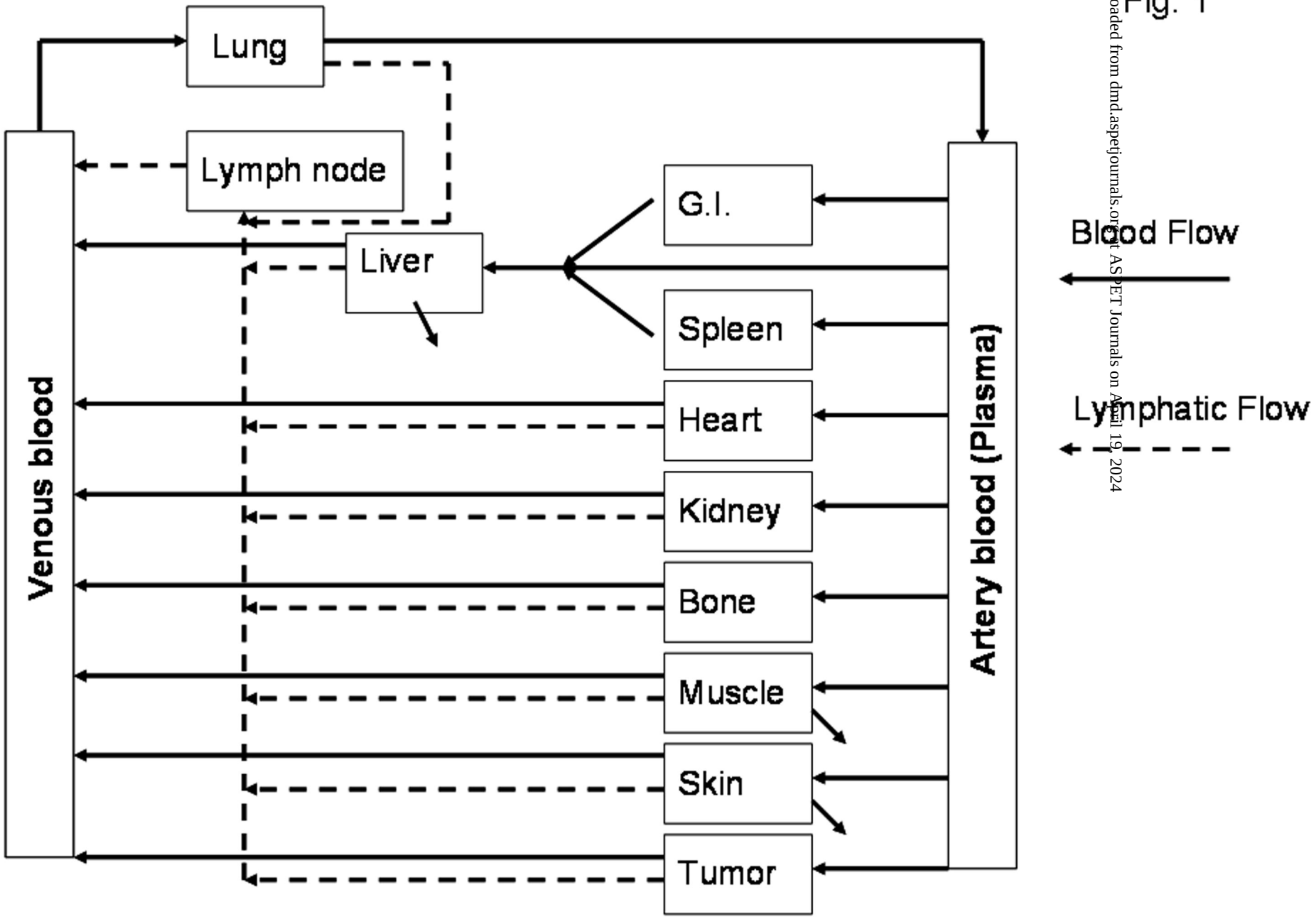

Fig 2A

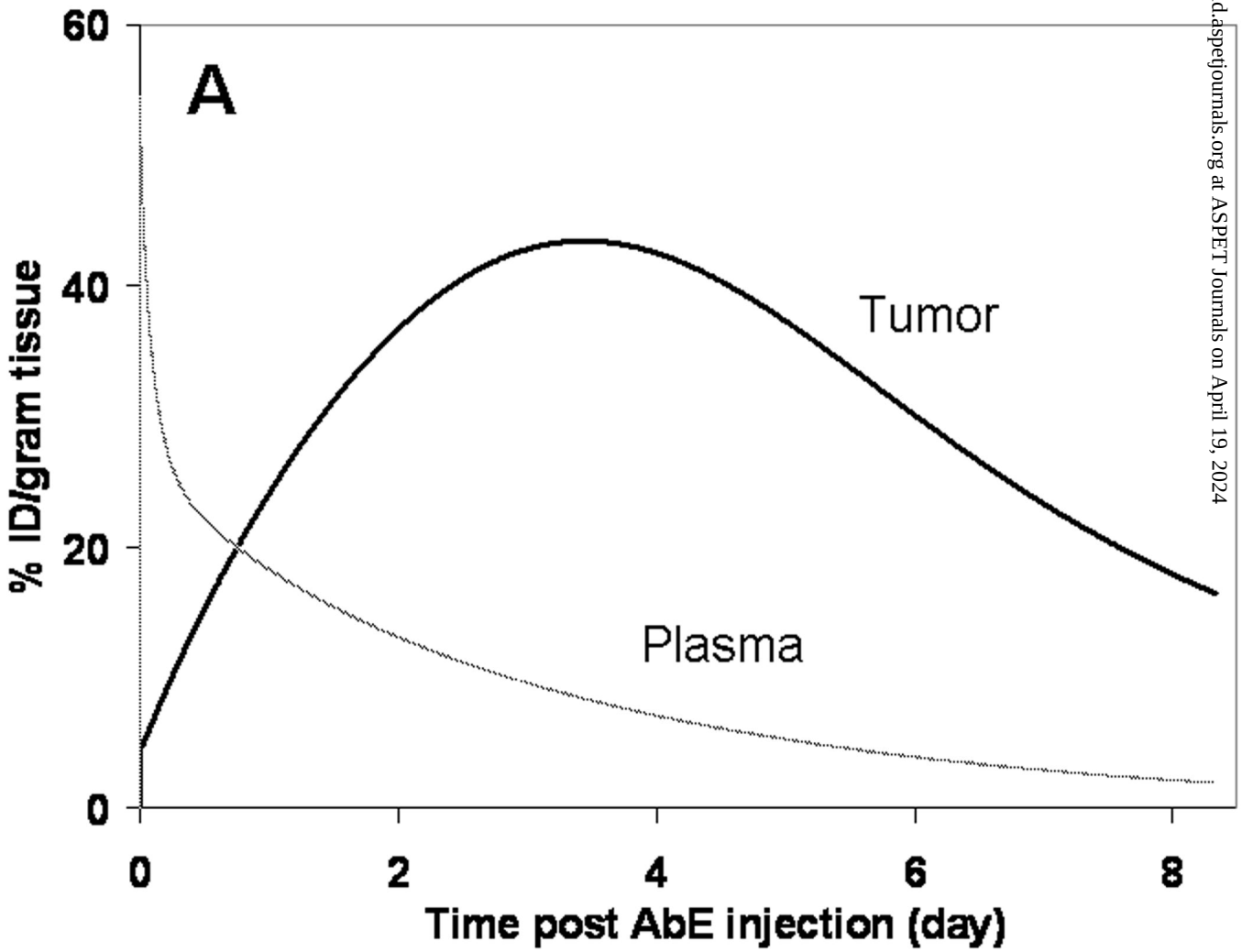

Fig. 2B

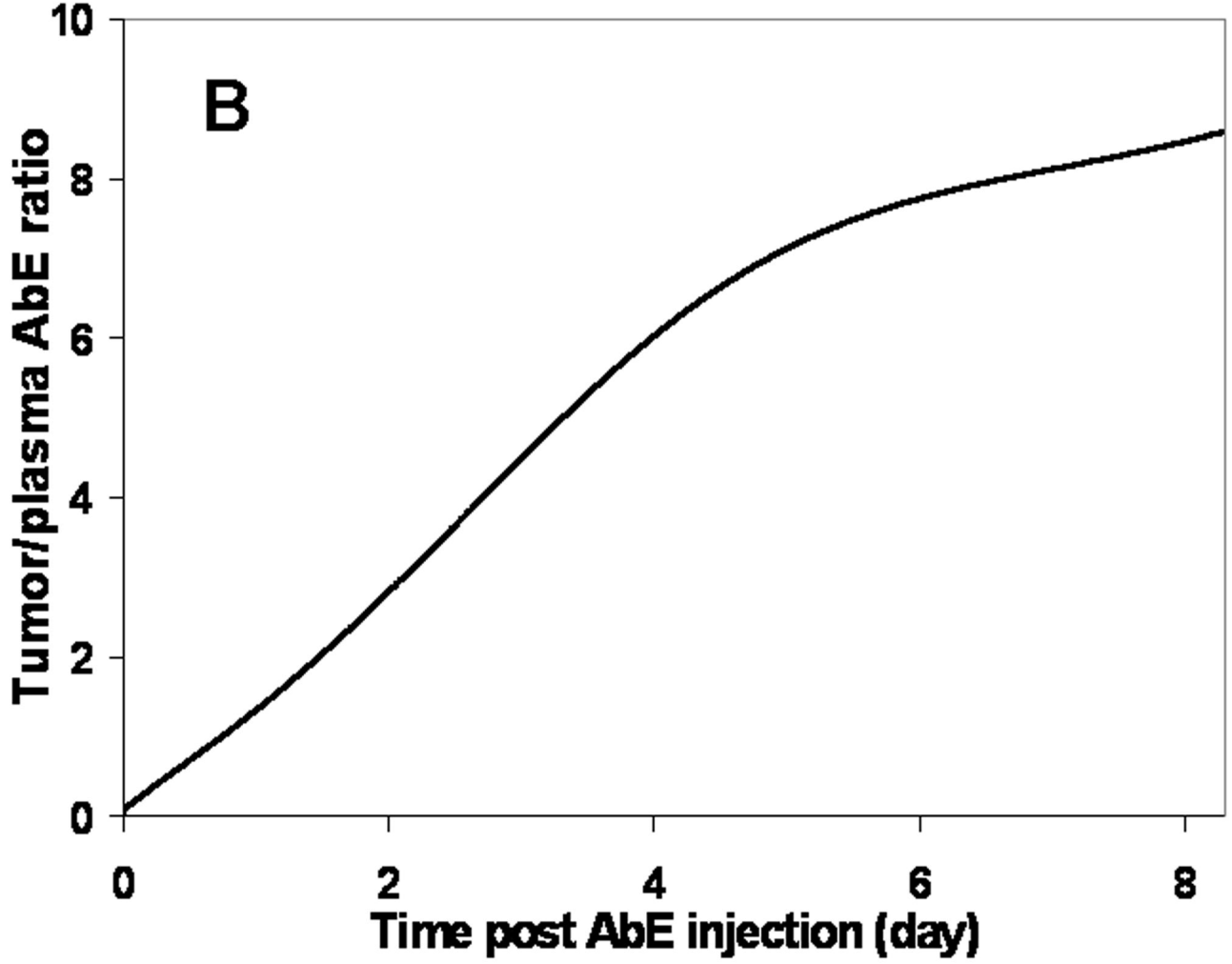

Fig. 2C

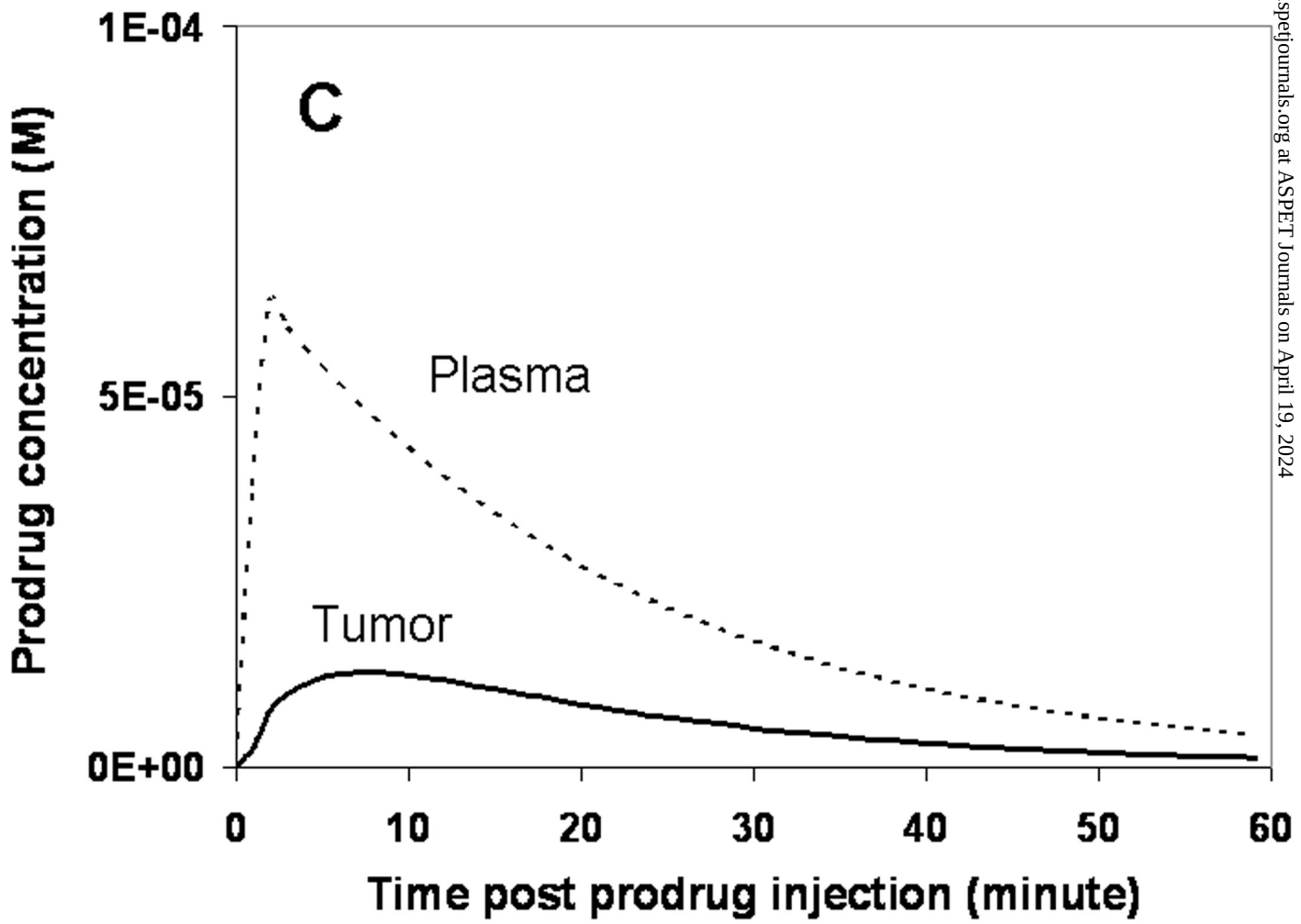

Fig. 2D

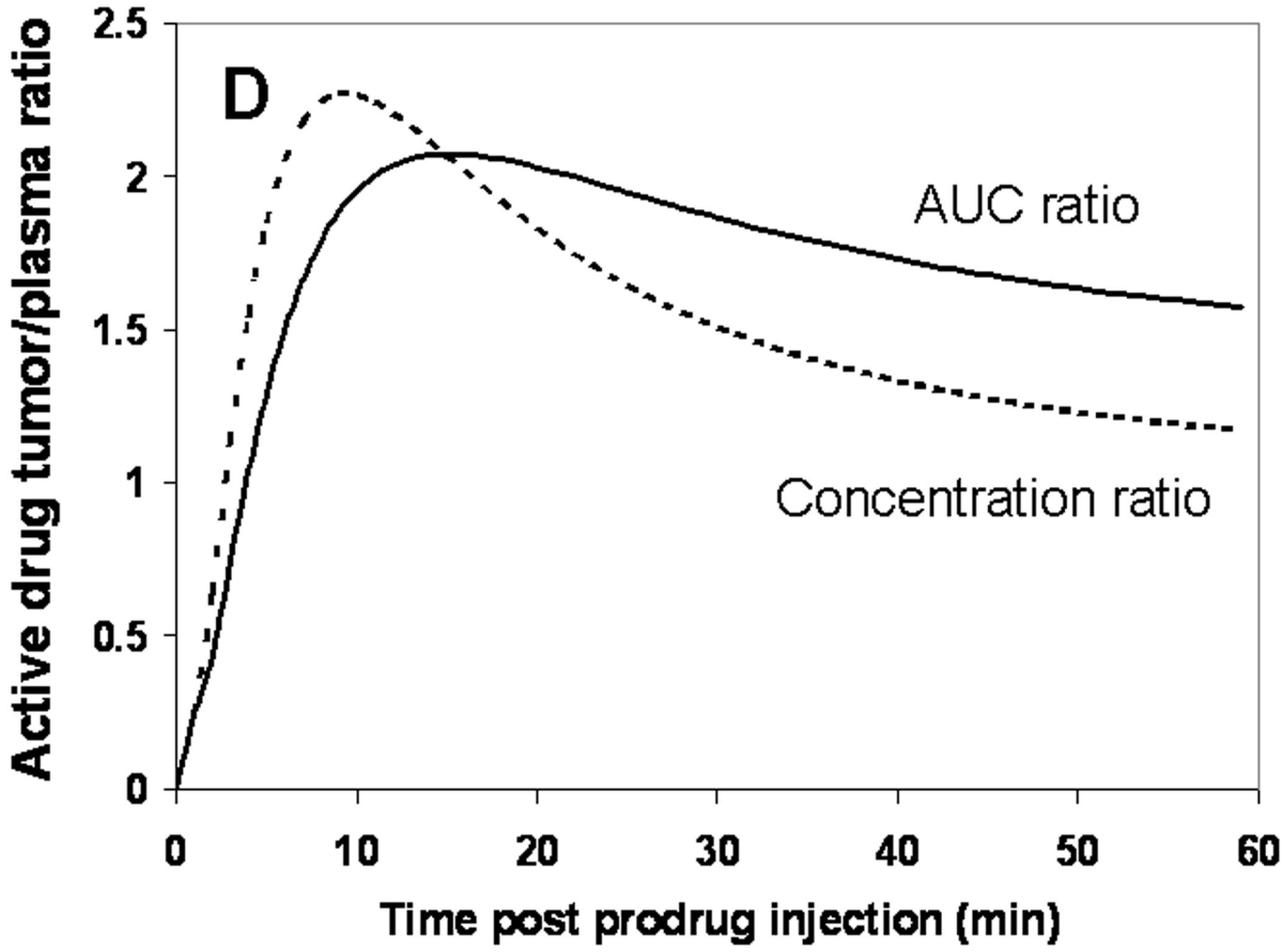

Fig. 3A

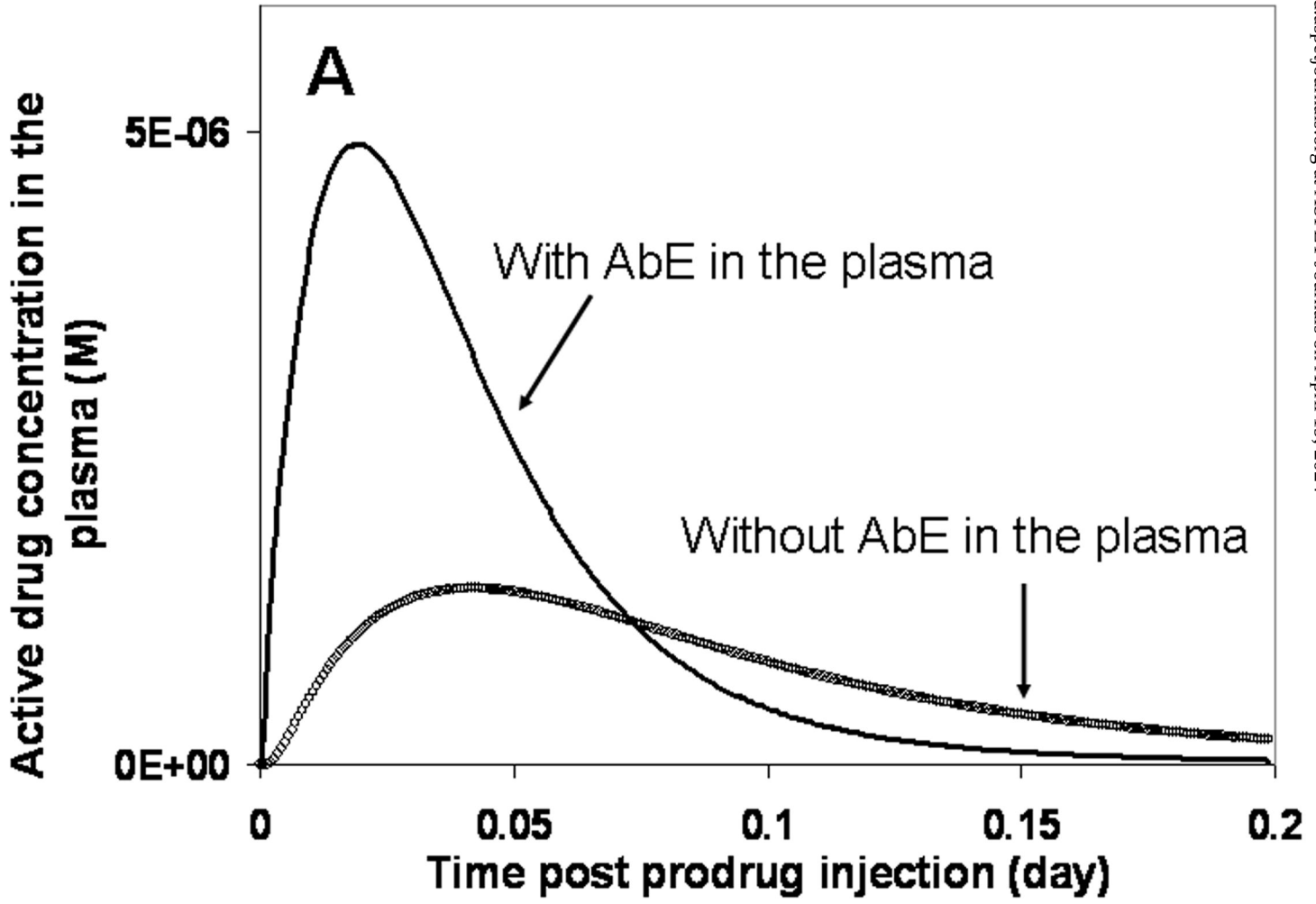

Fig. 3B

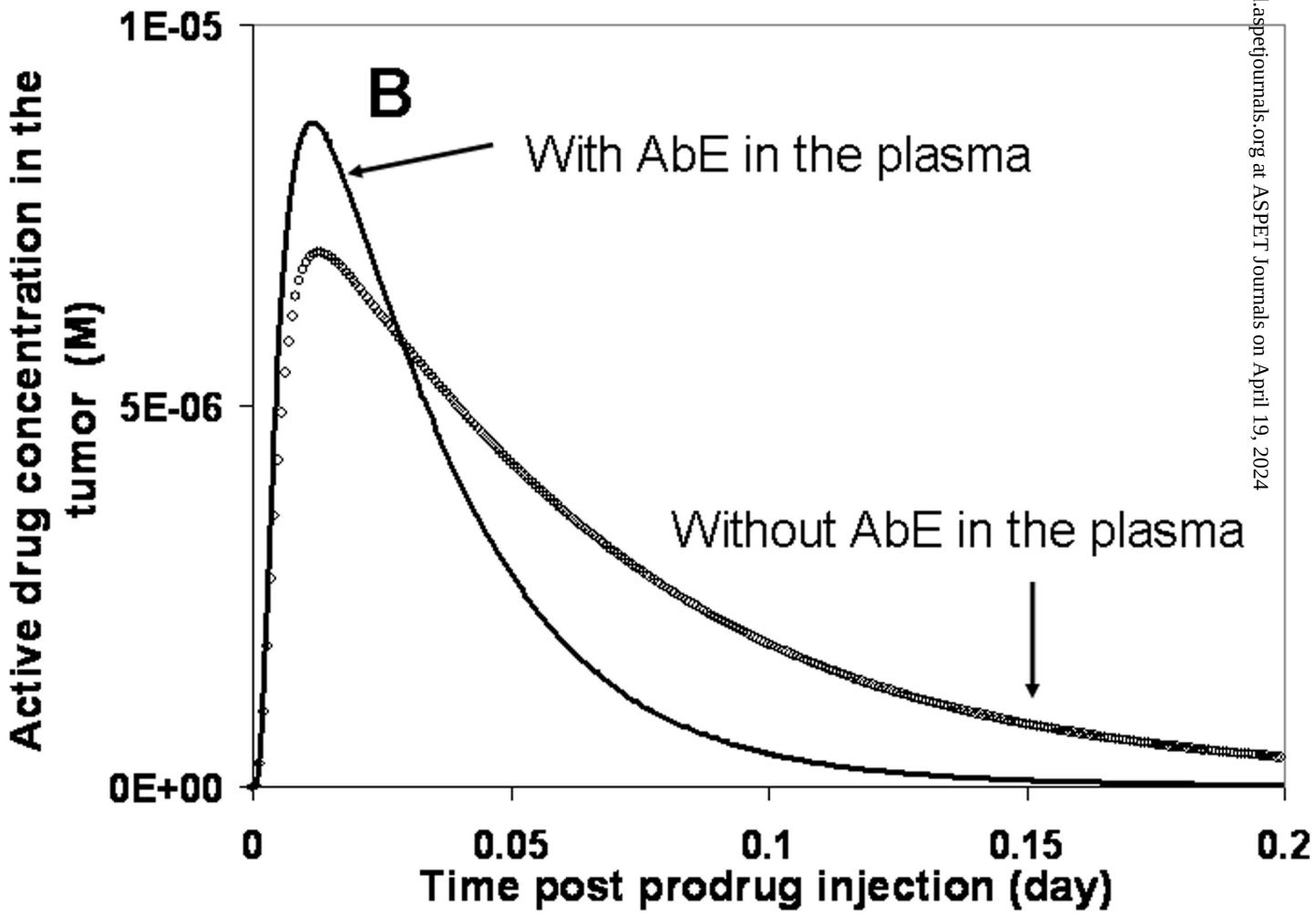

Fig. 3C

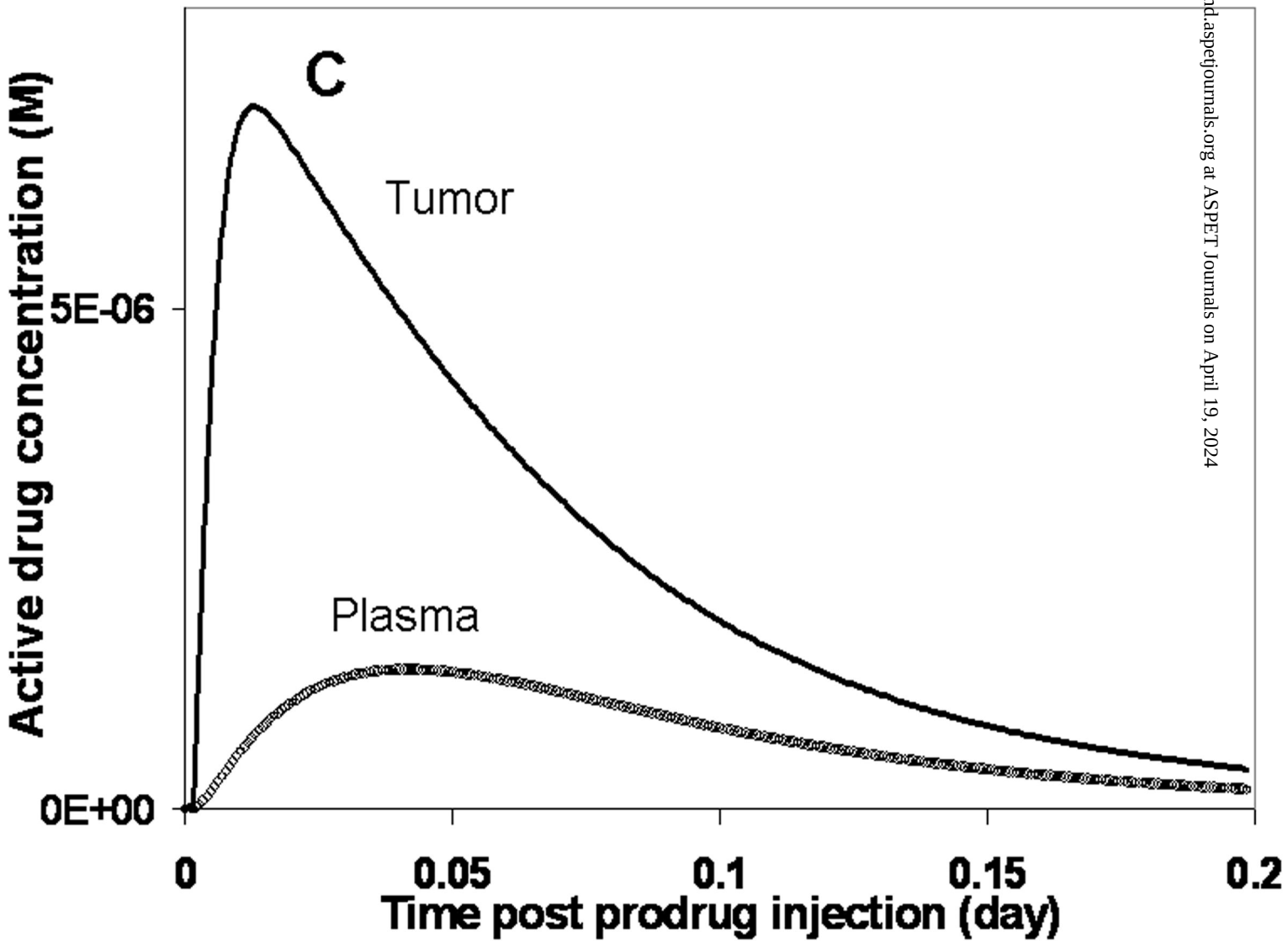

Fig. 4A

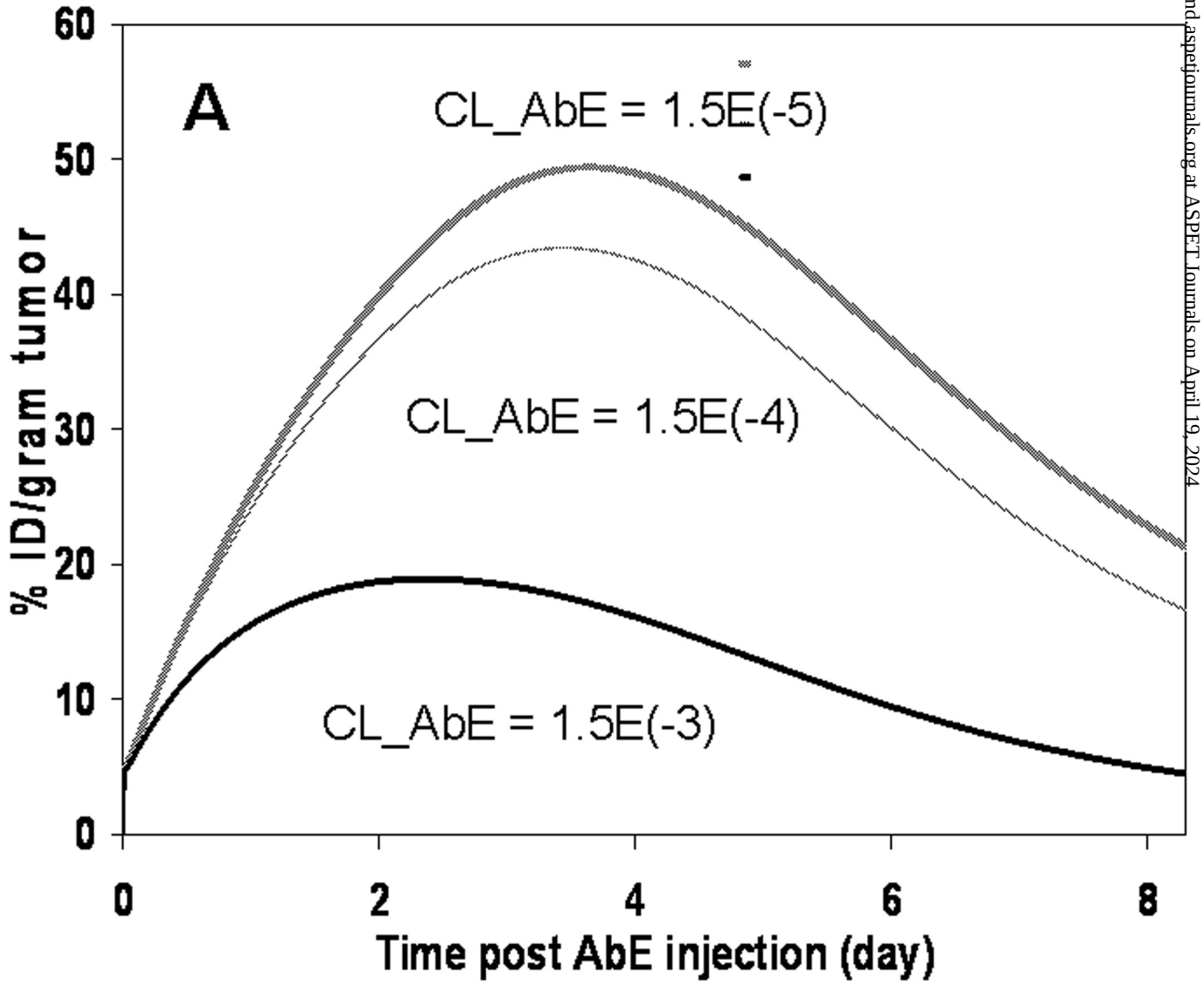

Fig. 4B

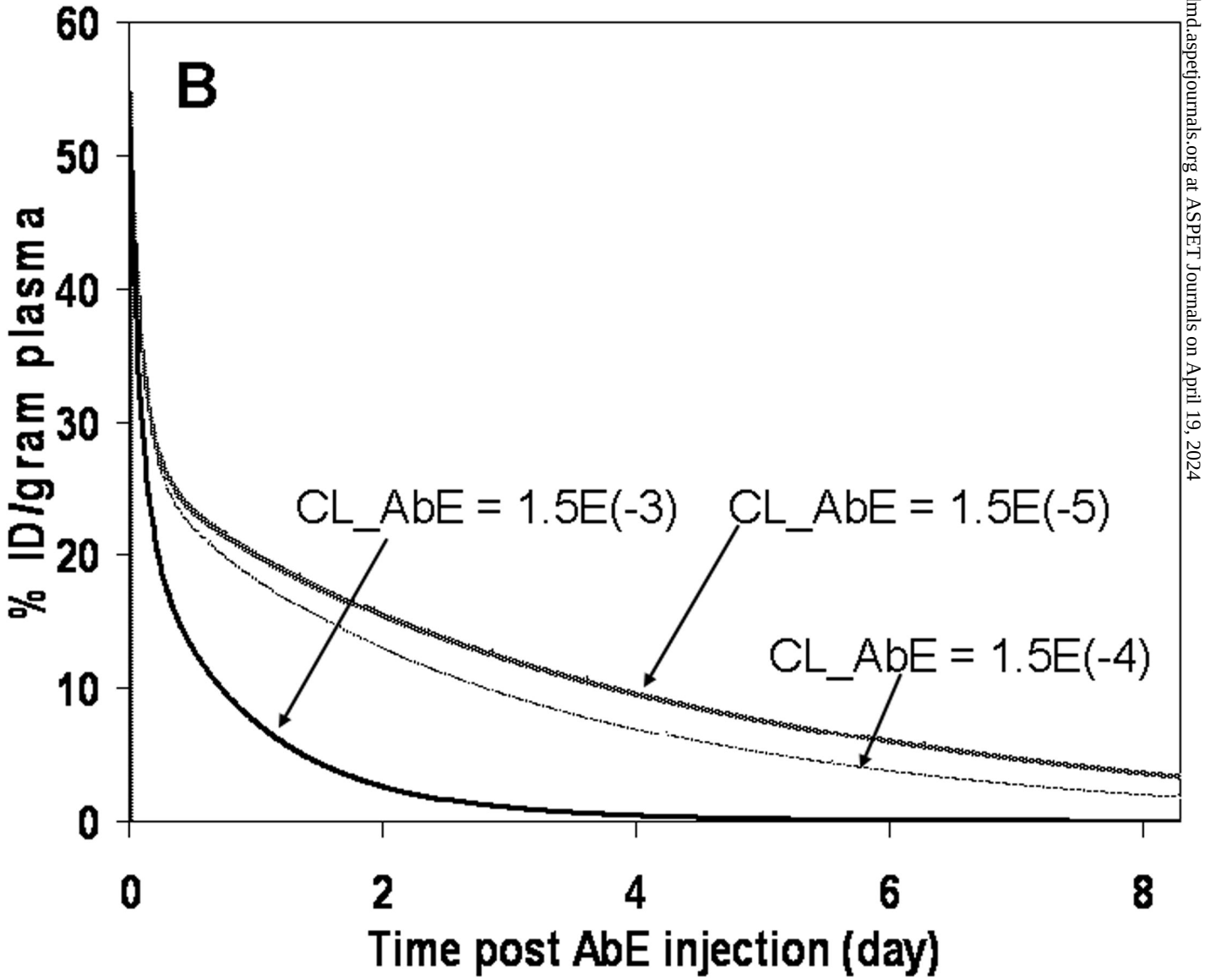

Fig. 4C

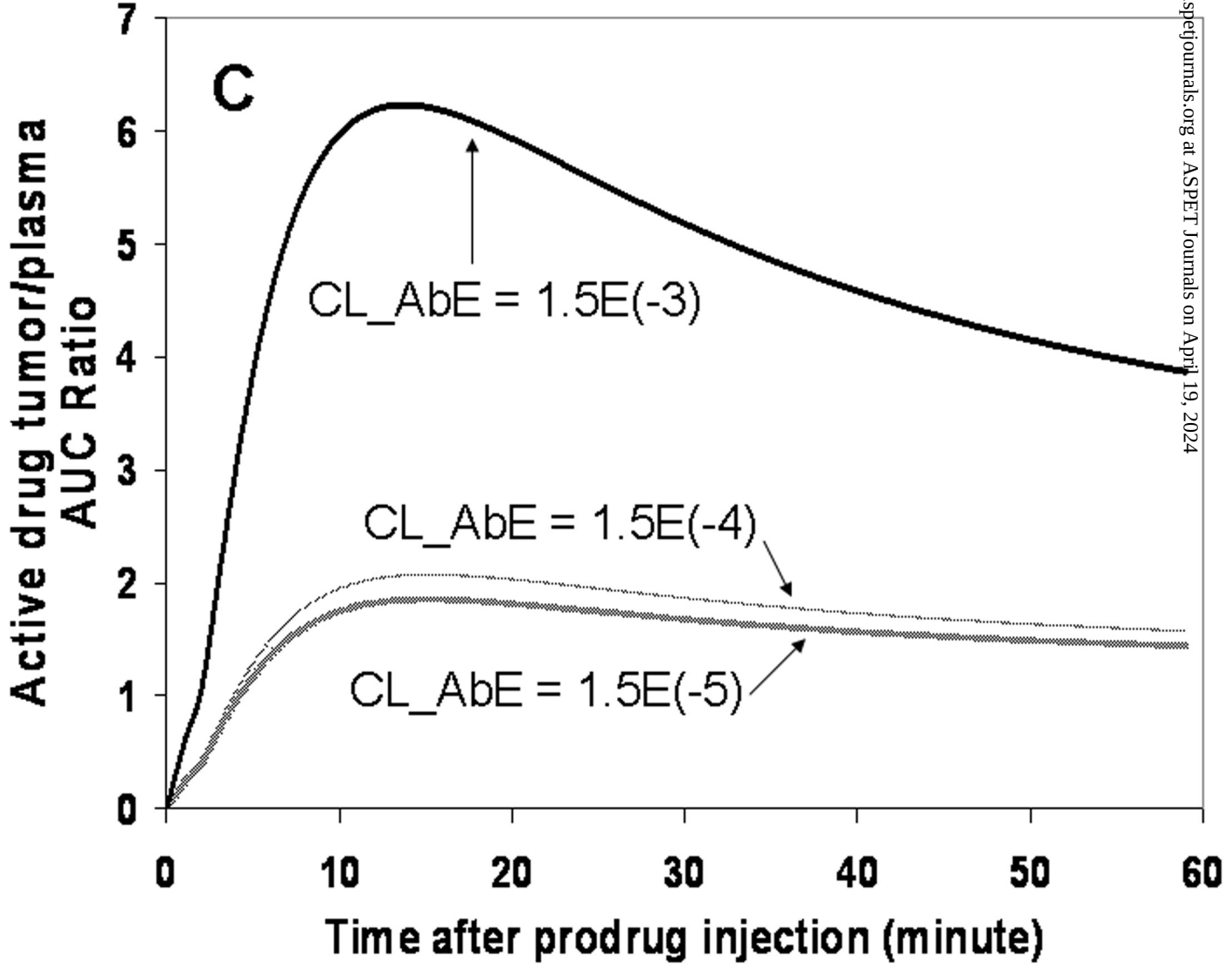

Fig. 5A

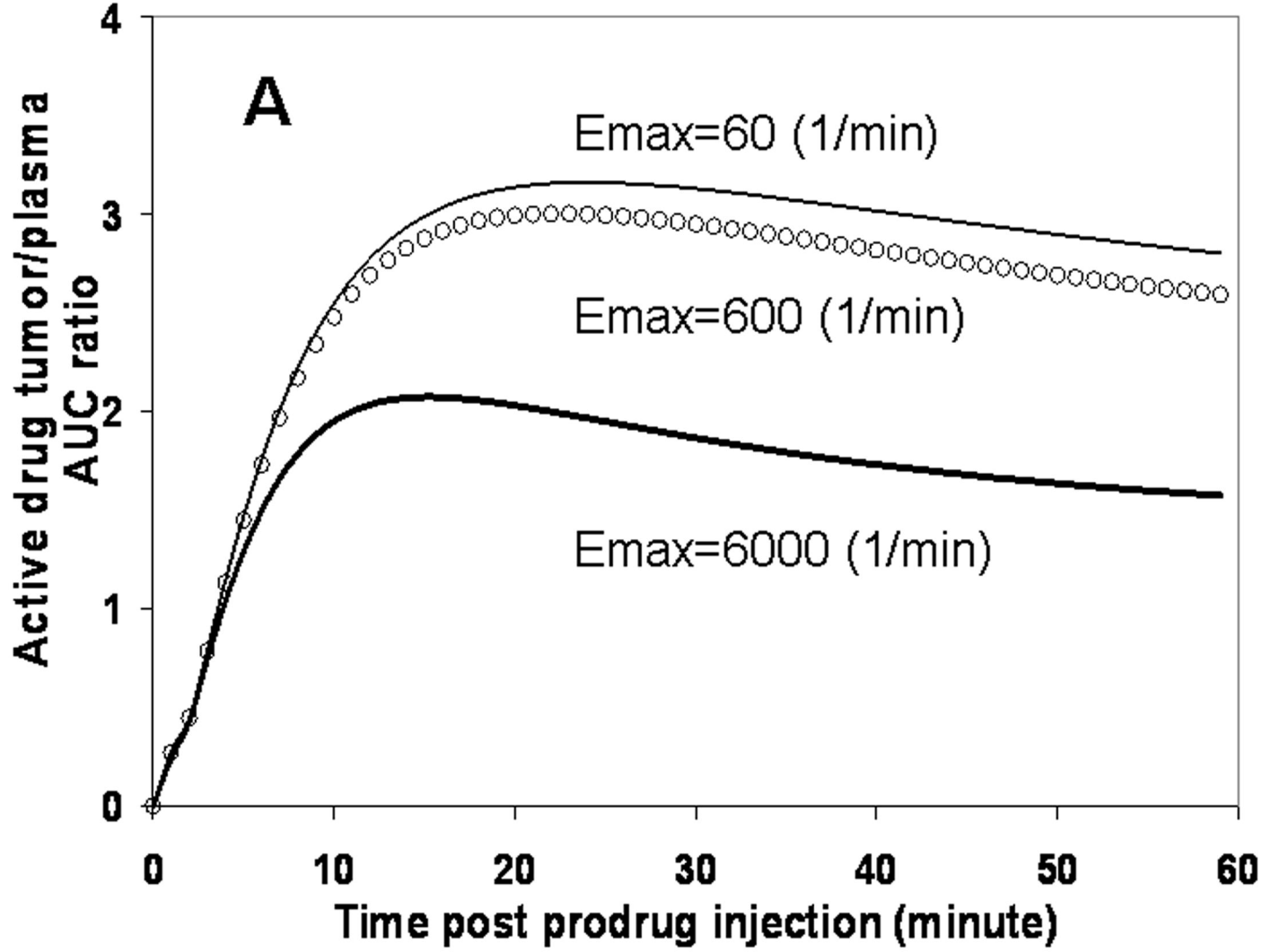

Fig. 5B

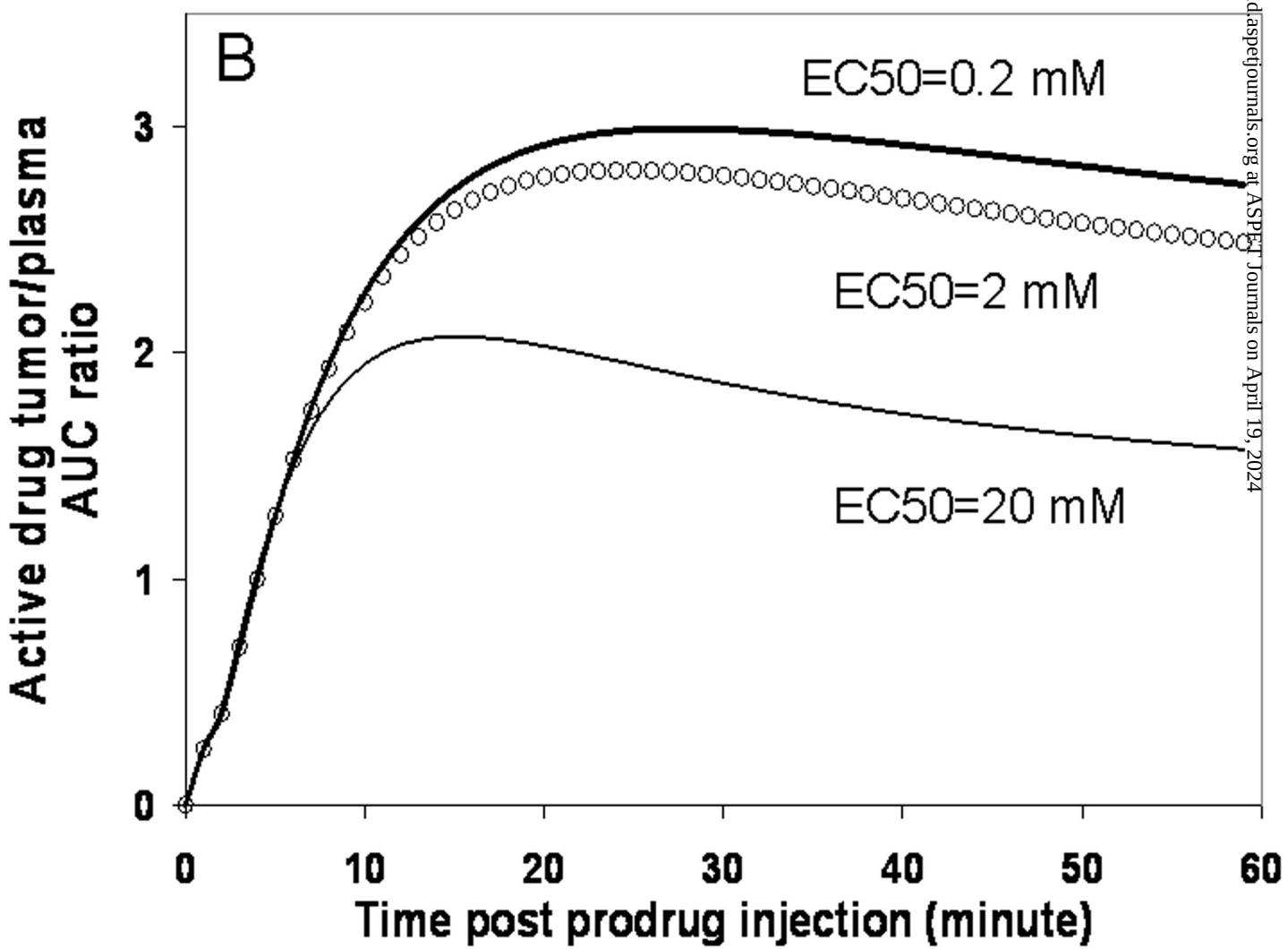

Fig. 5C

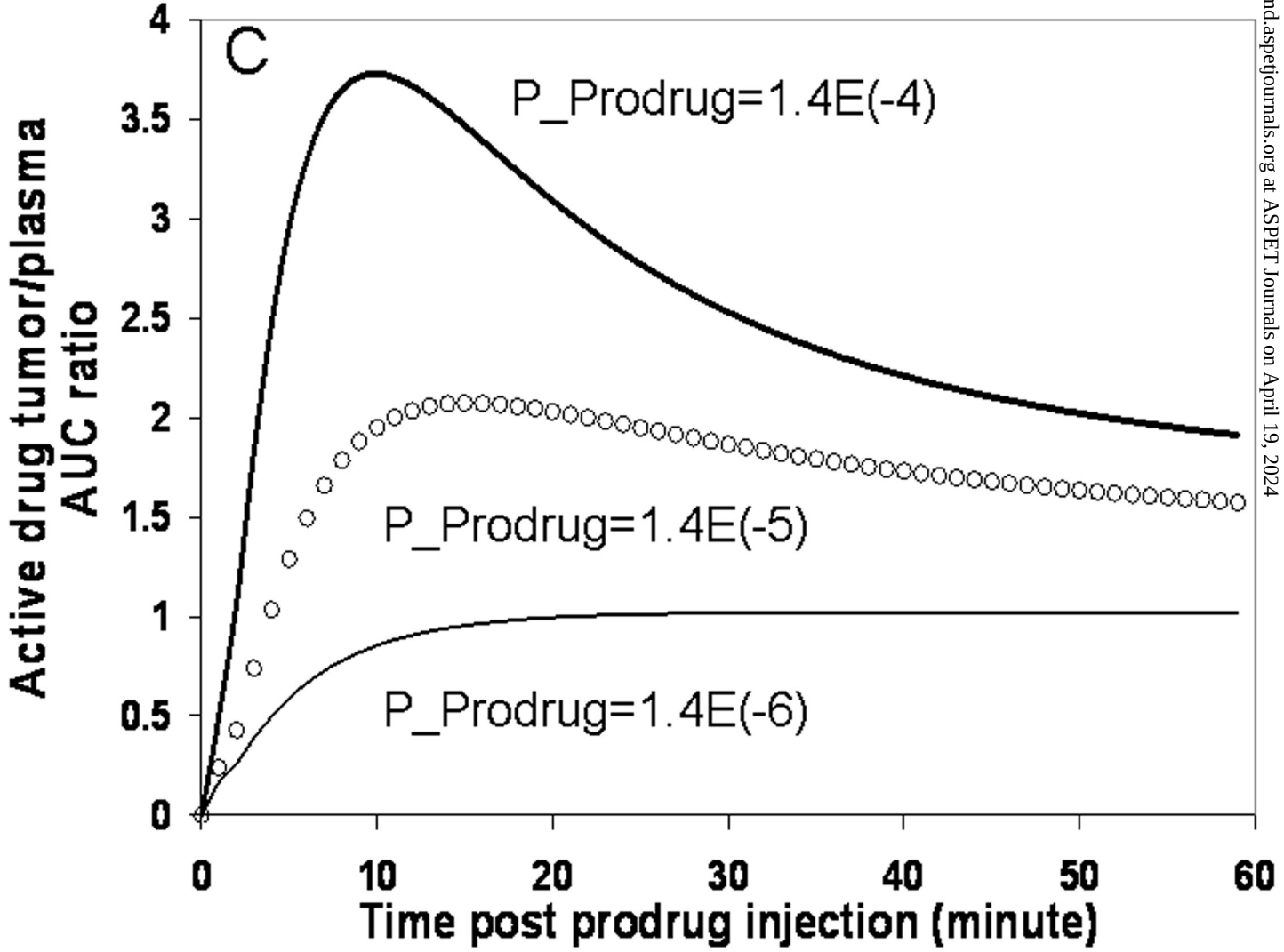

Fig. 5D

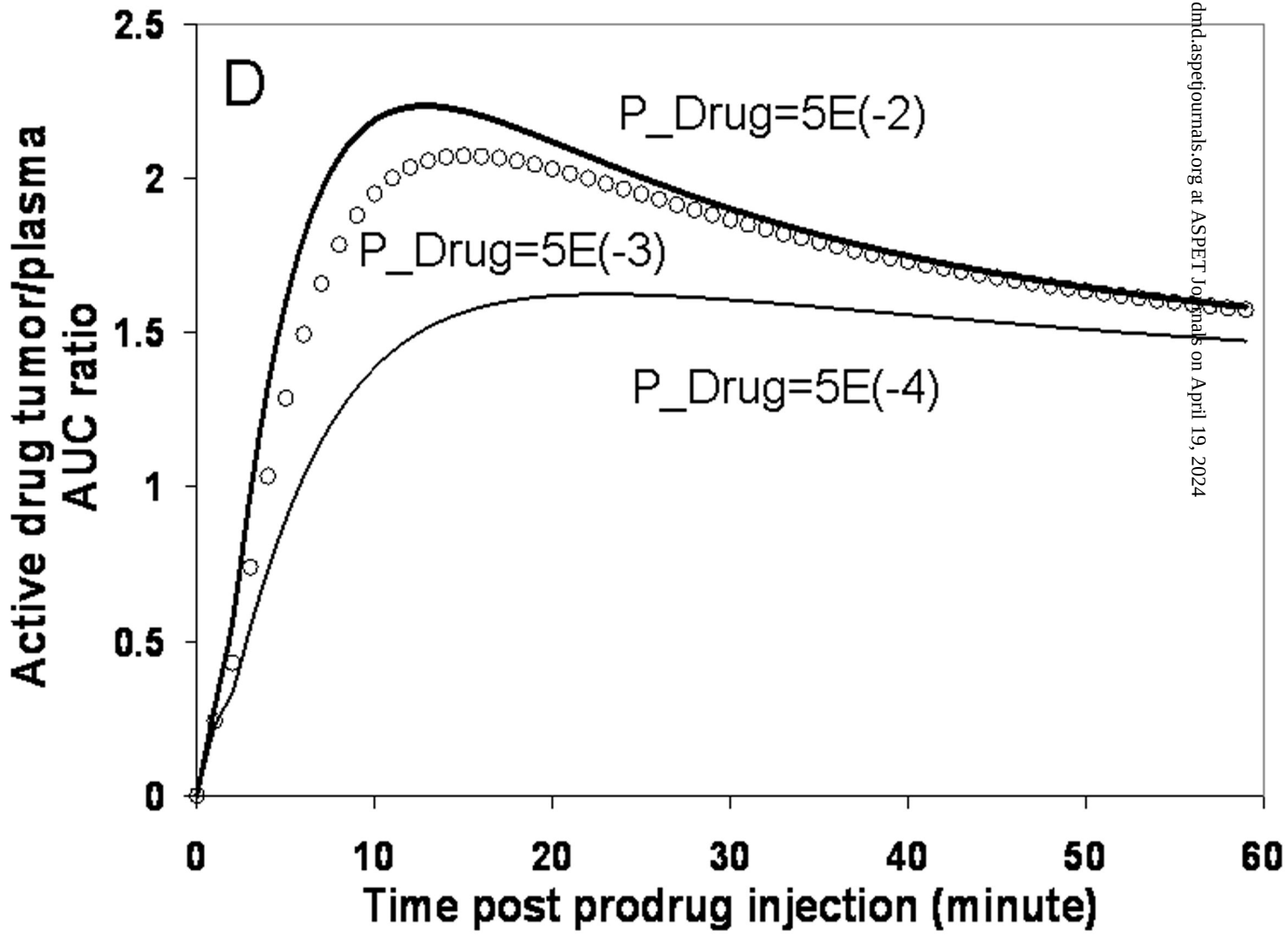

Fig. 5E

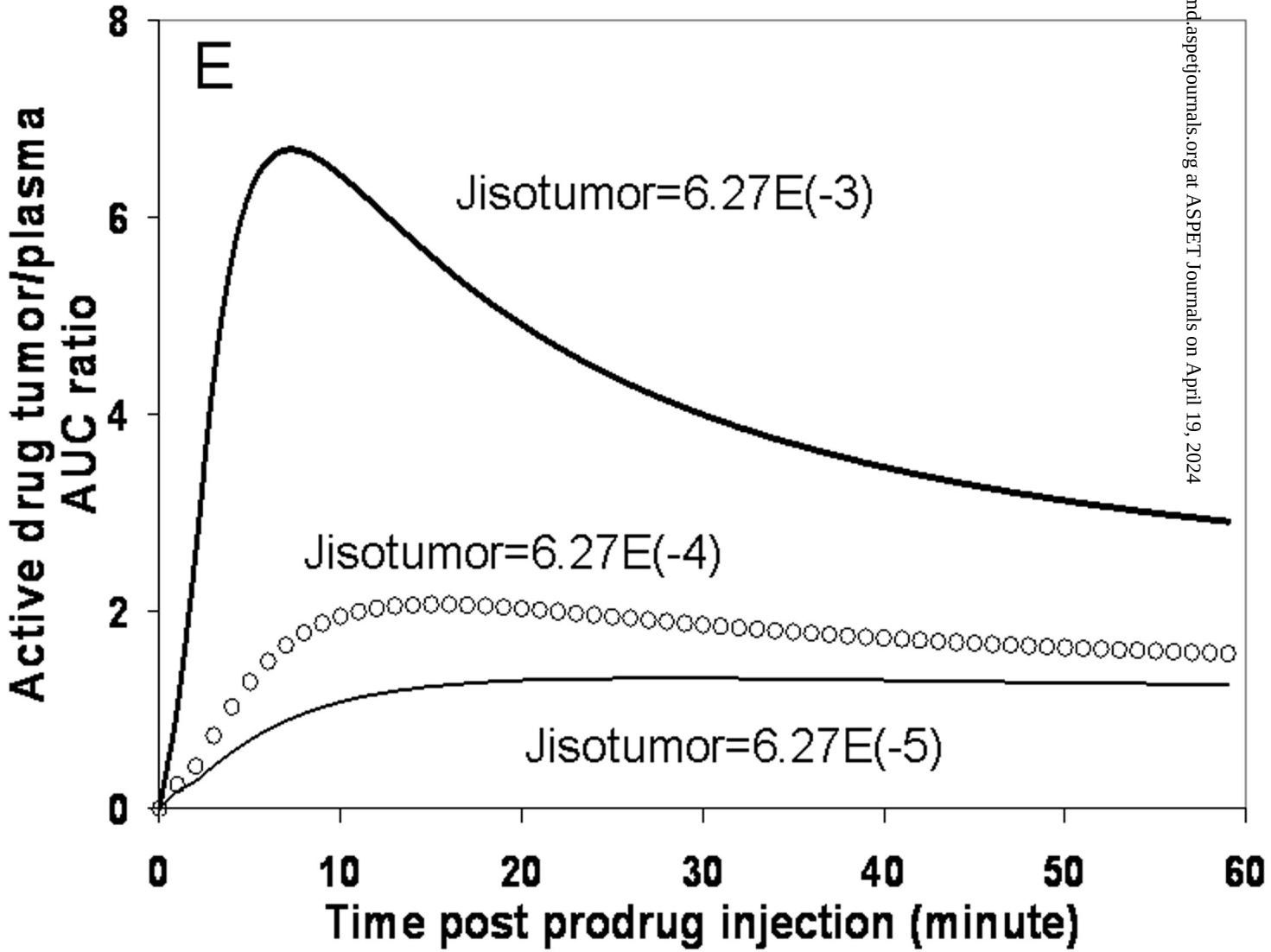

Fig 6

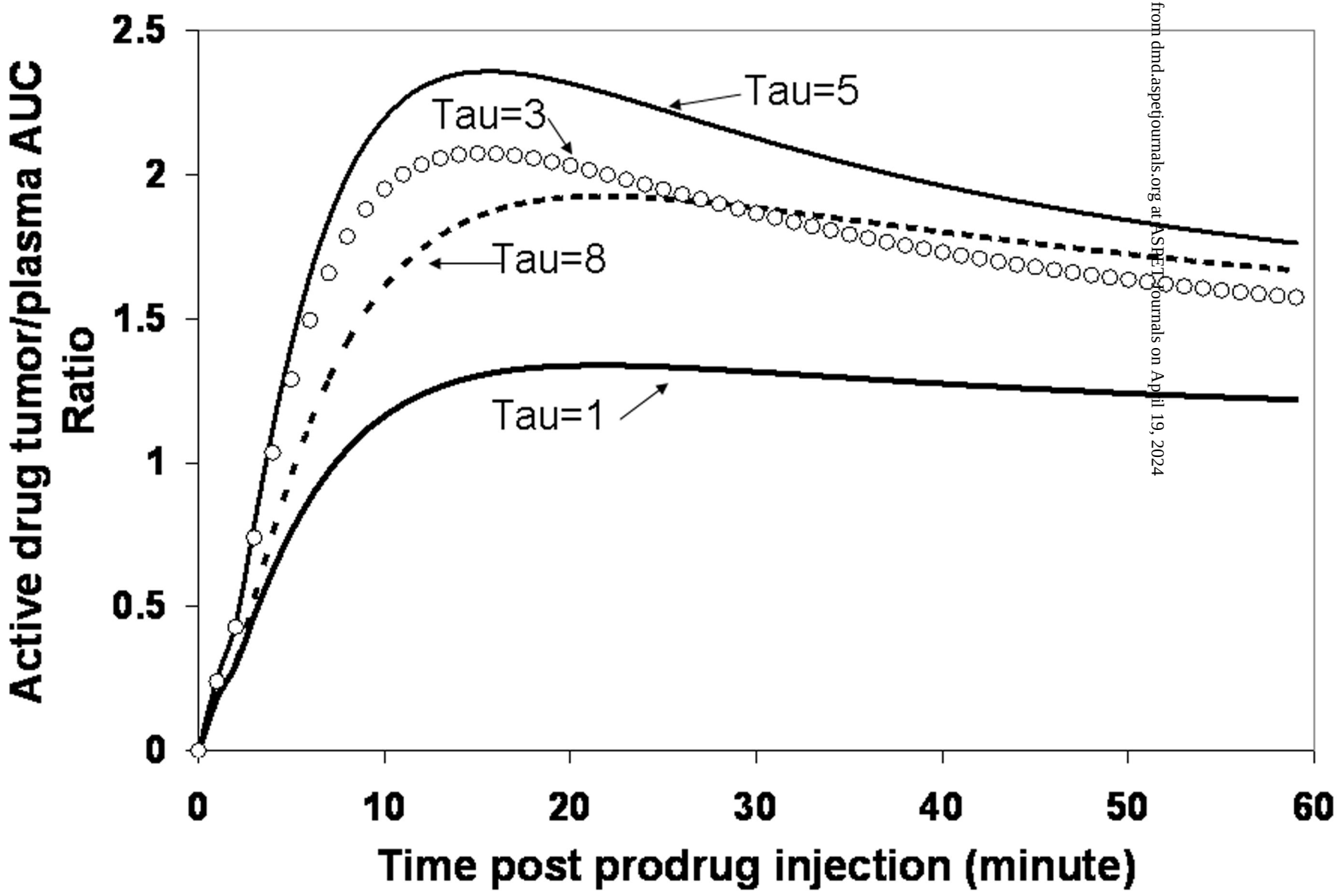

Fig. 7A

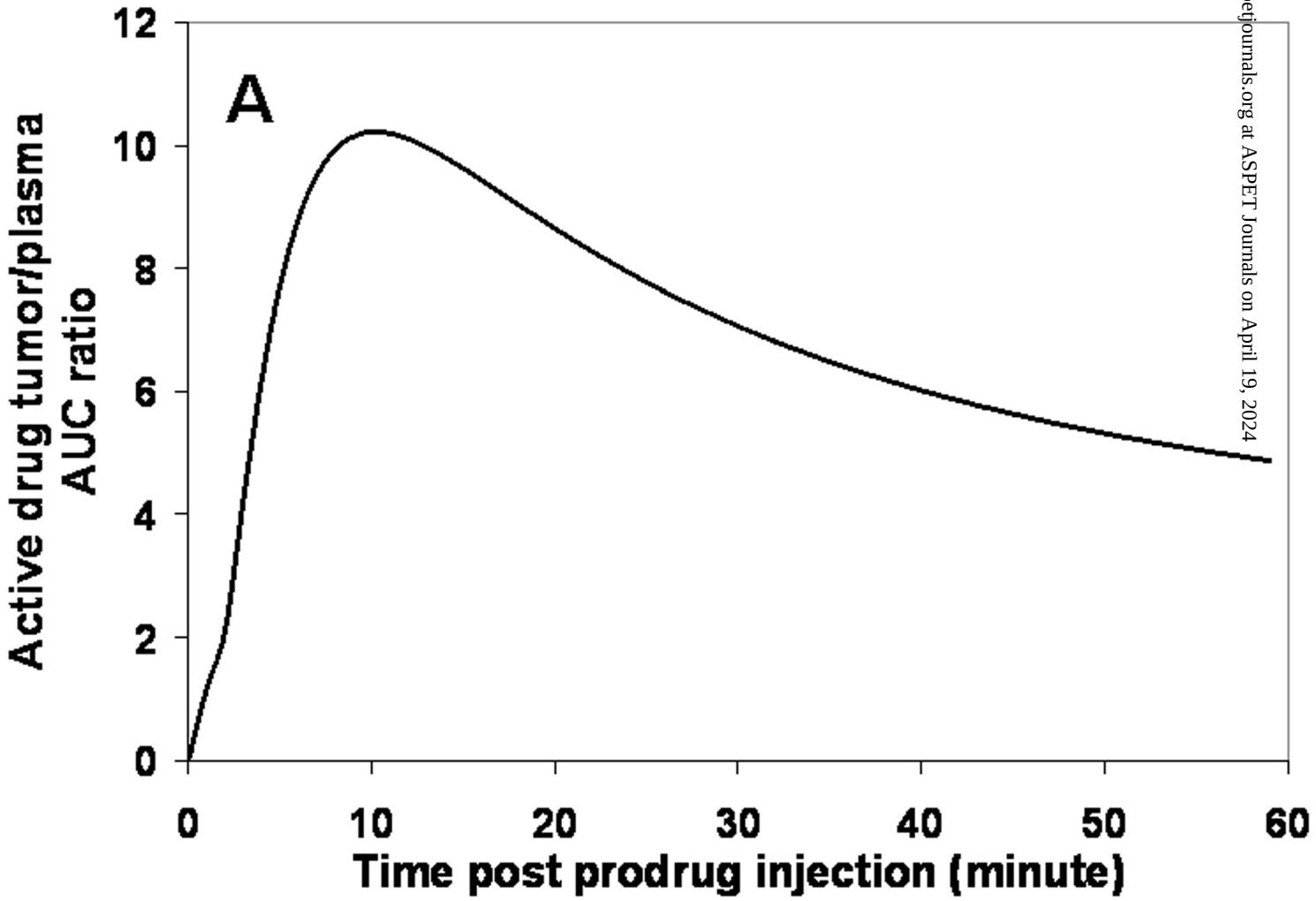

Fig. 7B

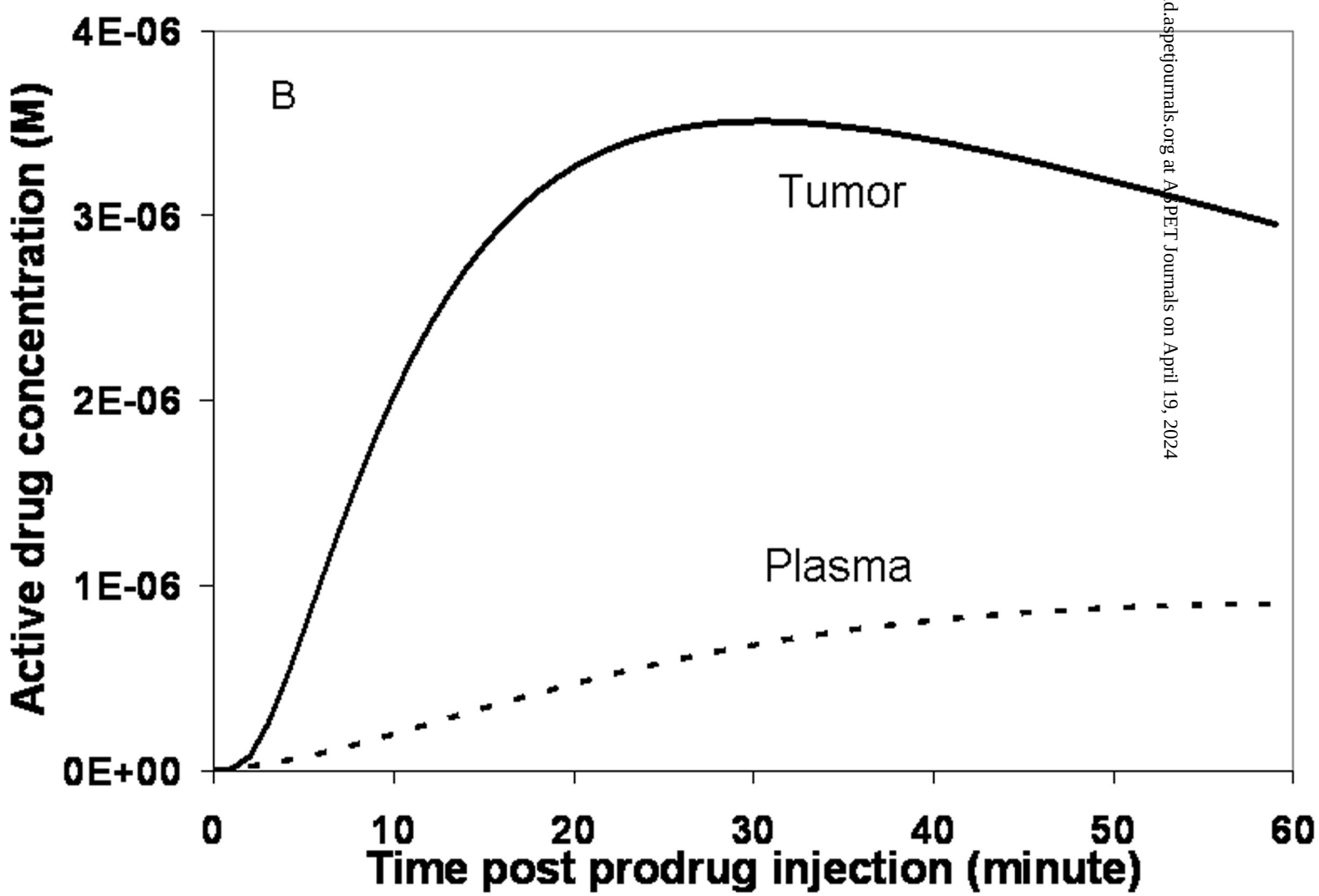

Fig. 8A

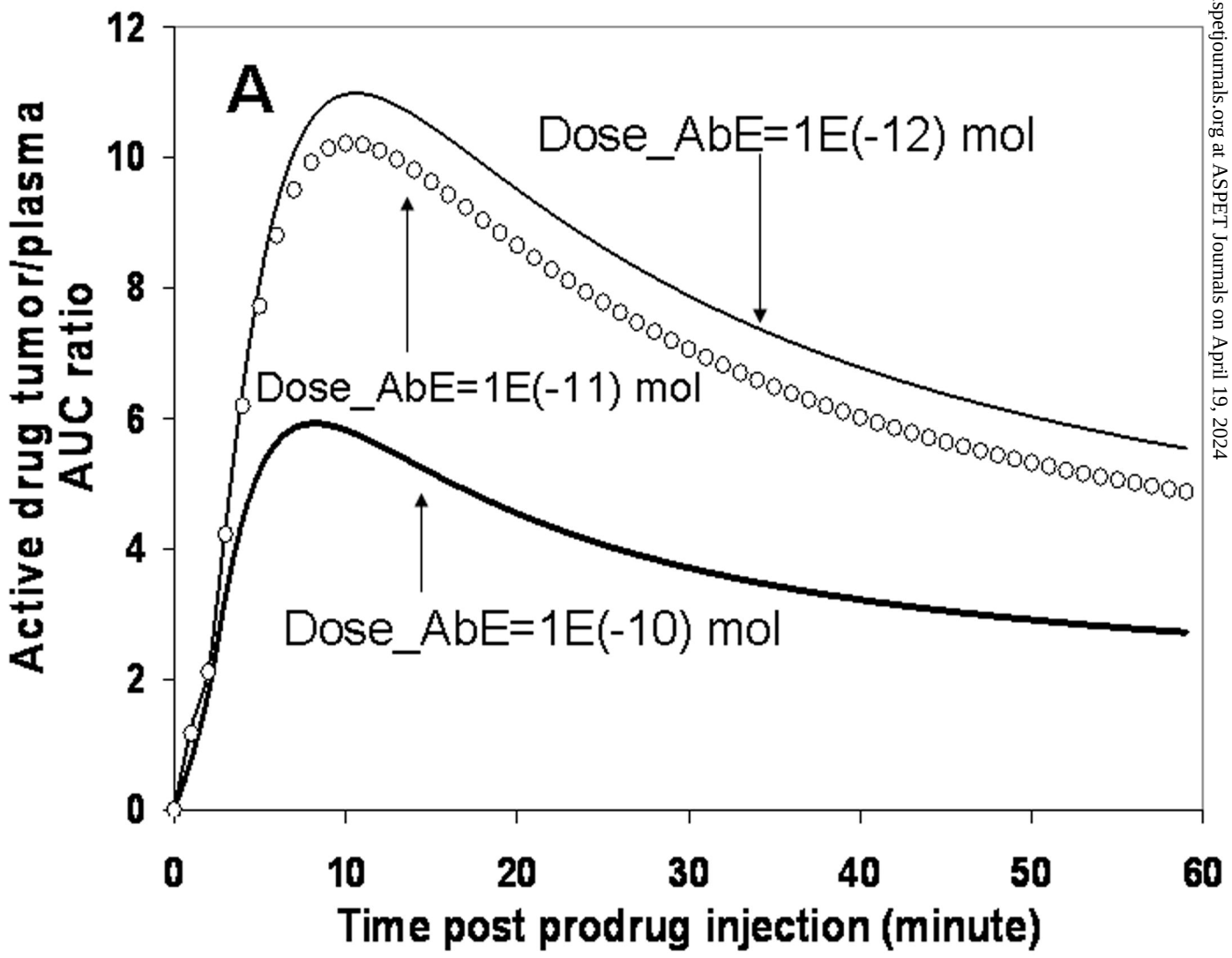

Fig. 8B

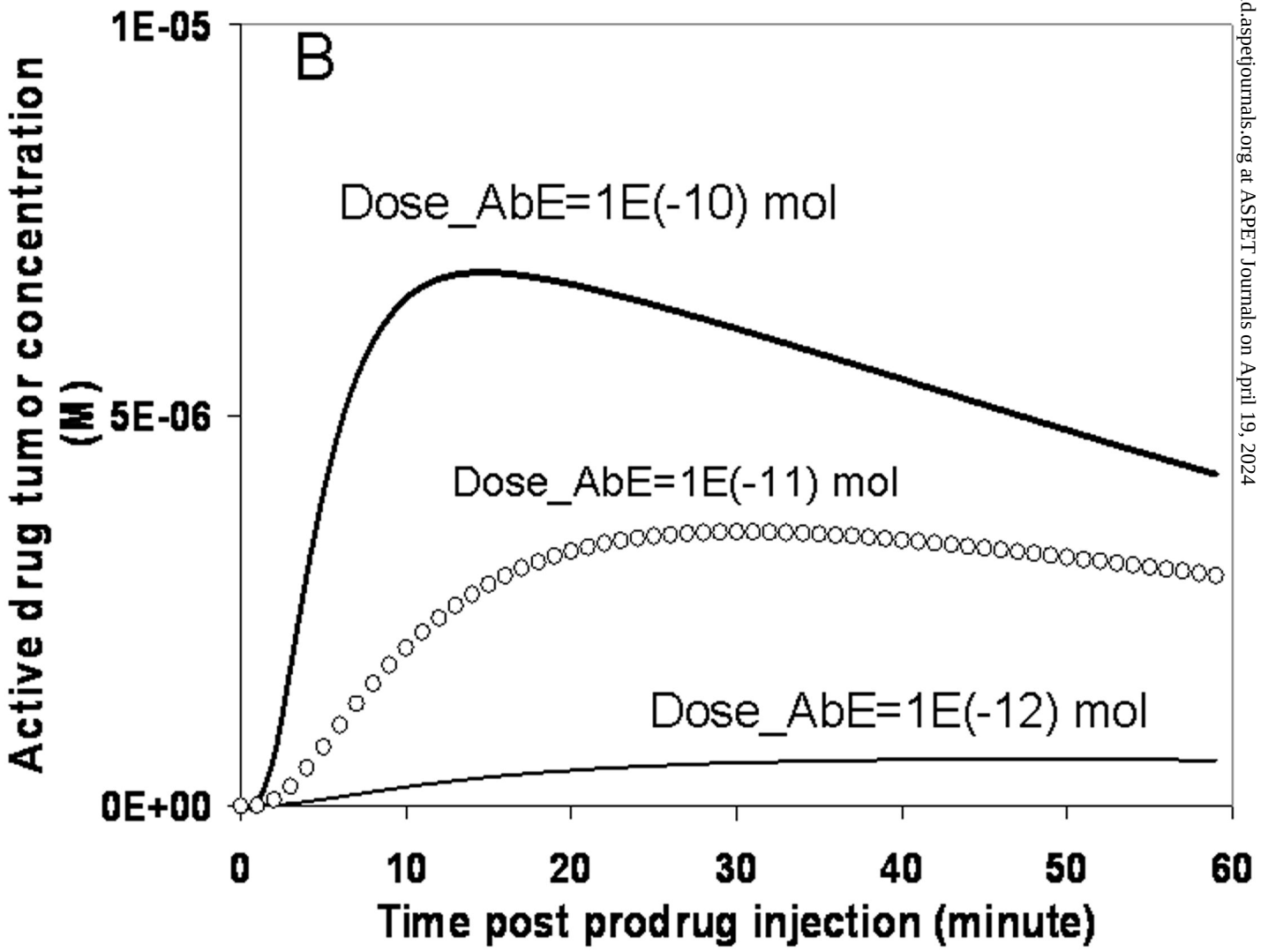

Fig. 8C

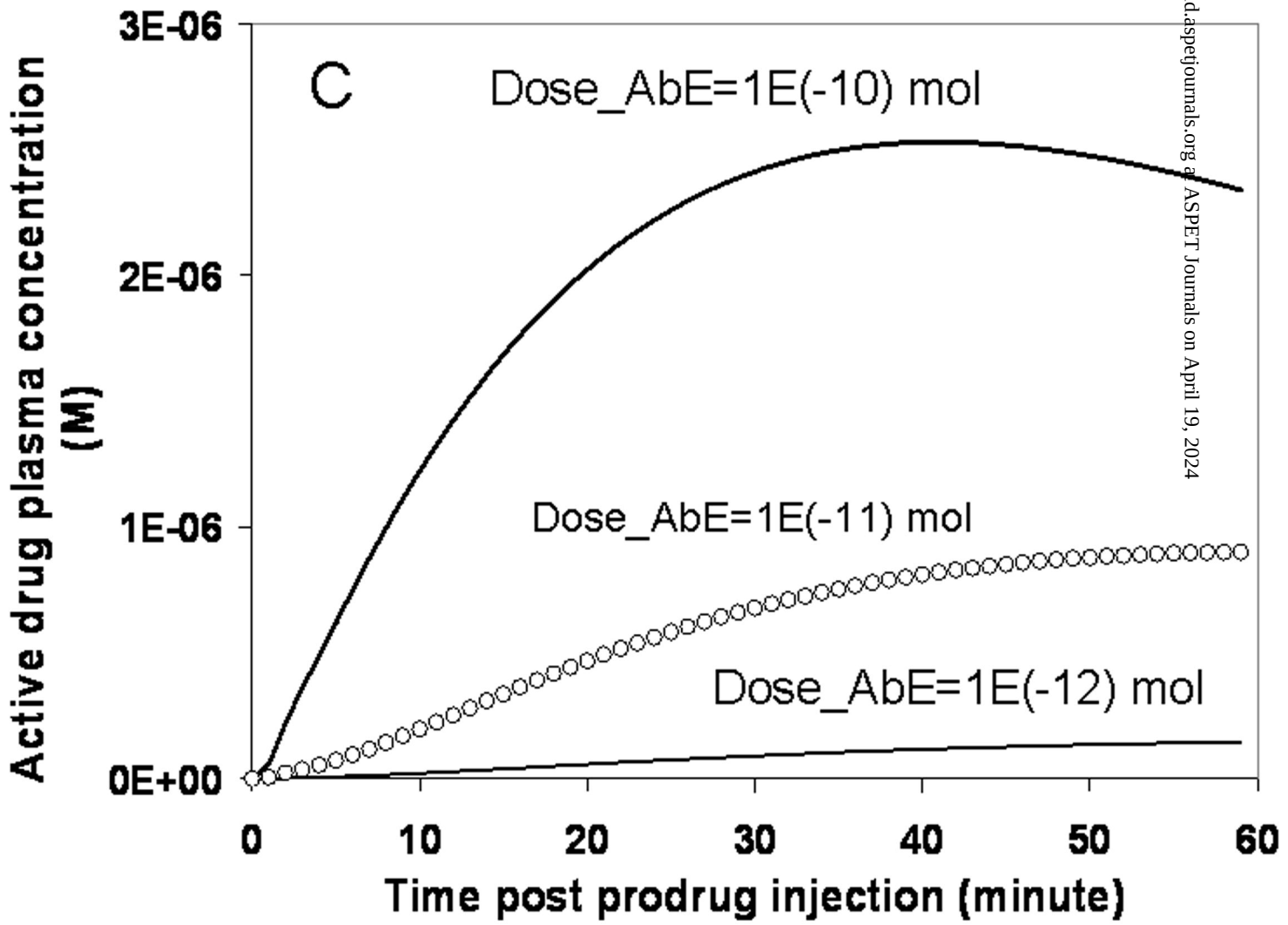

Fig. 8D

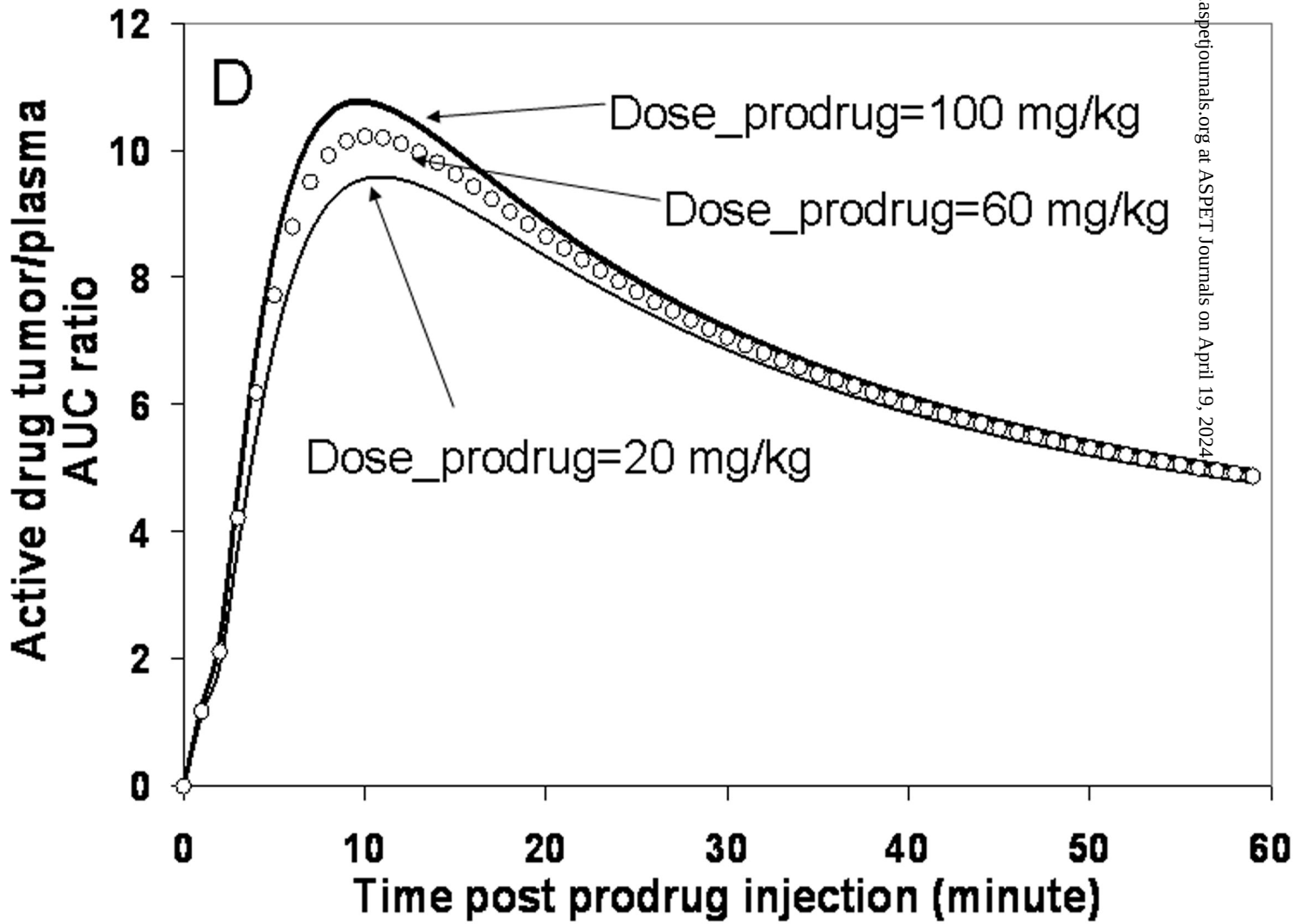

Fig. 8E

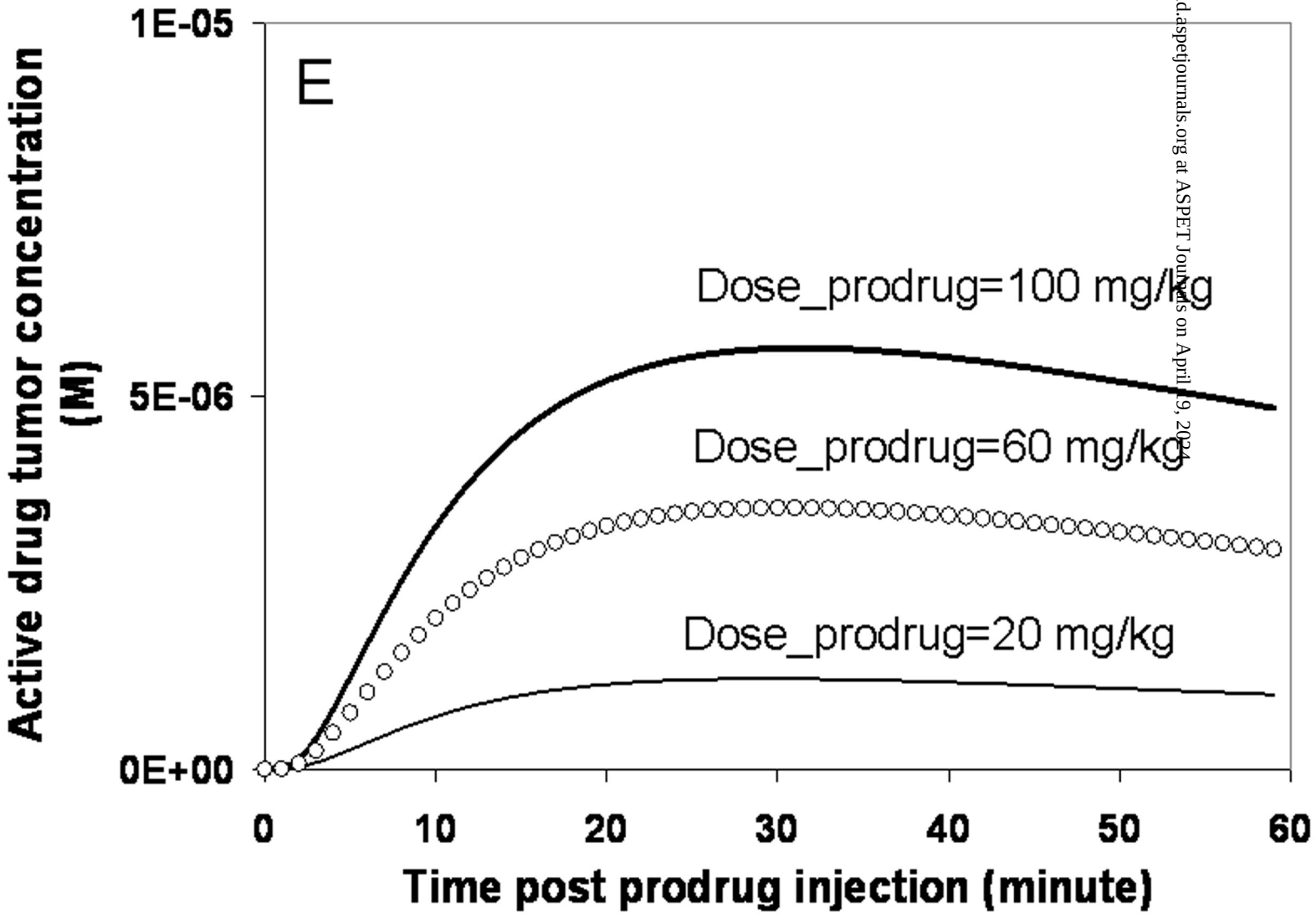

Fig. 8F

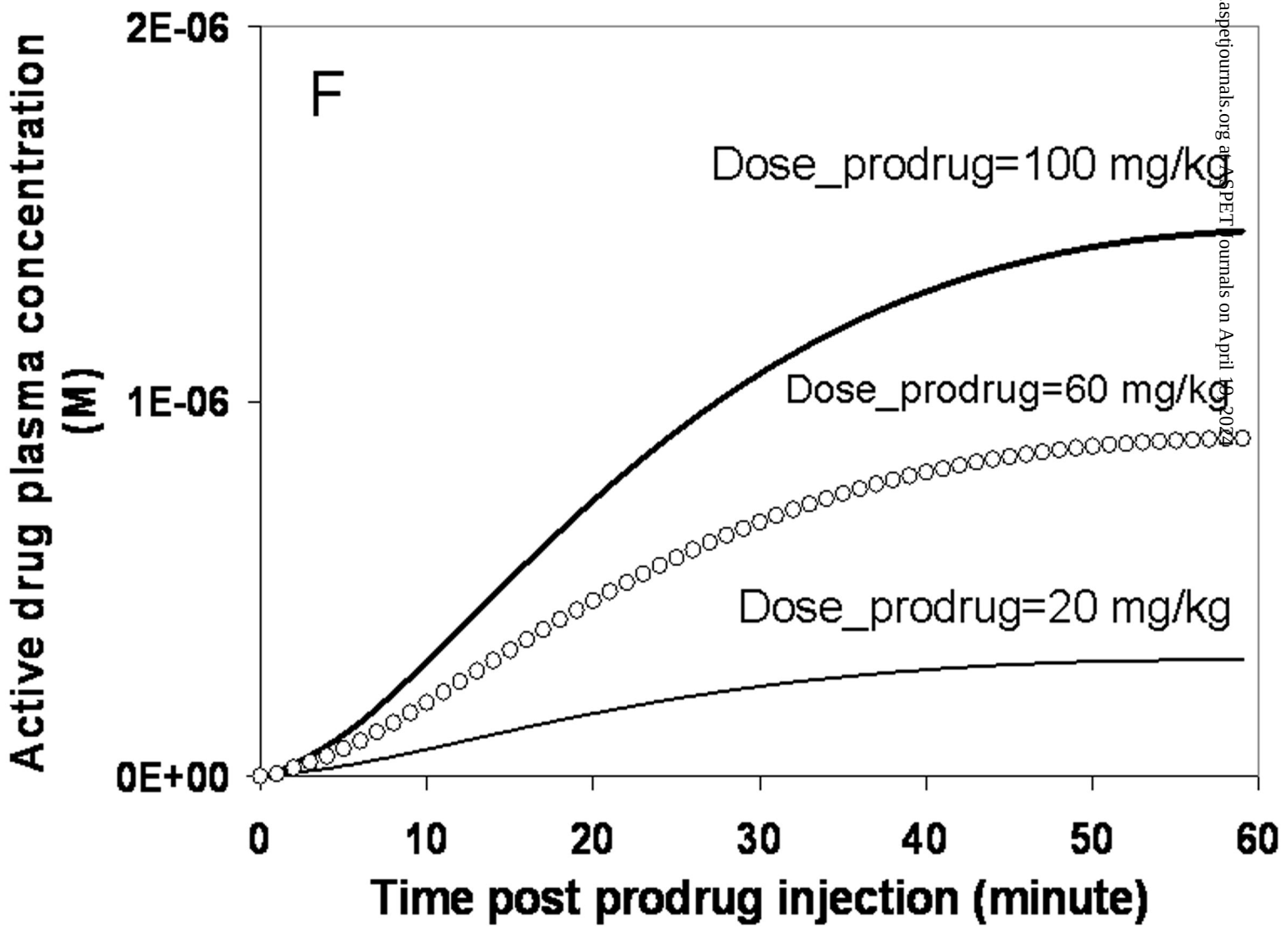

DMD Fast Forward. Published on March 20, 2008 as DOI: 10.1124/dmd.107.019182
This article has not been copyedited and formatted. The final version may differ from this version.

Appendix A: Nomenclature

Qorgan: Plasma flow rate of each organ (ml/min)

Lorgan: Lymph flow rate of each organ (ml/min/gram)

Jiso,organ: Fluid recirculation flow rate for each organ (=flow rate through large pore to the interstitial space for L=0; ml/min/gram)

Massorgan: Organ weight (gram)

Vvorgan:vascular space of each organ (ml)

Viorgan: interstitial space of each organ (ml)

Vorgan: total volume of each organ (ml)

σL, σS: osmotic reflection coefficient for large and small pores, respectively

αL, αS: fraction of extravasation via large and small pores, respectively

PSLorgan, PSSorgan: Permeability-surface area product for each organ (ml/min) for large and small pores, respectively

PeLorgan, PeSorgan: Peclet number, ratio of convection to diffusion across large and small pores (=J(1-σ)/PS)

JLorgan, JSorgan: Transcapillary fluid flow rate (vascular->interstitial) for each organ (ml/min) via large and small pores, respectively

Bmax: Maximum tumor-associated antigen concentration inside tumor tissue (mol/ml)

KfCEA: association rate constants for the binding of antibodies (ml/mol/min).

KrCEA: dissociation rate constants for the binding of antibodies (1/min)

FcRntot: total FcRn binding capacity in the skin and muscle (mol/ml)

KintFcRn: nonspecific internalization rate constant of free antibody into endosome for binding to FcRn sites (1/min)

DMD Fast Forward. Published on March 20, 2008 as DOI: 10.1124/dmd.107.019182
This article has not been copyedited and formatted. The final version may differ from this version.

KrecFcRn: recycling rate of FcRn bound antibody back to vascular space (1/min)

konFcRn: binding constant for IgG-FcRn interaction (ml/mol/min)

koffFcRn: dissociation constant for IgG-FcRn interaction (1/min)

kdegFcRn: degradation rate constant of unbound endosomal IgG (1/min)

CLdegLiver: clearance of antibody-enzyme conjugate (AbE) from liver (ml/min)

Cpl: AbE concentration in plasma (mol/ml)

Cv, organ: AbE concentration in the vascular space of each organ (mol/ml)

Cif, organ: free AbE concentration in the interstitial space of each organ (mol/ml)

Cib, organ: bound AbE concentration in the interstitial space of each specified organ (mol/ml)

Cef,organ: free AbE concentration in the endosome (mol/ml)

Ceb,organ: bound AbE concentration in the endosome with FcRn (mol/ml)

Ctot, organ: total AbE concentration in each organ (mol/ml)

fub_ProDrug, fub_Drug: unbound free fractions in blood for prodrug and active prodrug, respectively

Emax_ProDrug: maximum rate constant for converting prodrug to active drug by antibody-enzyme conjugate (AbE) (1/min)

EC50_ProDrug: EC50 for converting prodrug to active drug by antibody-enzyme conjugate (AbE) (mol/ml)

Clint_ProDrug, Clint_Drug: liver intrinsic clearance for prodrug and active, respectively (ml/min)

P_ProDrug, P_Drug: effective permeability coefficient for prodrug and active drug, respectively (1/min)

DMD Fast Forward. Published on March 20, 2008 as DOI: 10.1124/dmd.107.019182
This article has not been copyedited and formatted. The final version may differ from this version.

PS_ProDrug, PS_Drug: Permeability-area product for prodrug and active drug, respectively (ml/min)

Rprodrug,organ, Rdrug,organ: tissue to plasma concentration ratio of each organ for prodrug and active drug, respectively

Cpl_ProDrug, Cpl_Drug: plasma concentration for prodrug and active drug, respectively (mol/ml)

Cv_ProDrug, organ, Cv_Drug, organ: prodrug and active drug concentration in the vascular space of each organ (mol/ml)

Ci_ProDrug, organ, Ci_Drug, organ: prodrug and active drug concentration in the interstitial space of each organ (mol/ml)

Ctot_ProDrug, organ, Ctot_Drug, organ: total prodrug and active drug concentration in each organ (mol/ml)

AUC_Prodrug, organ, AUC_Drug, organ: AUC for prodrug and active drug in each organ (mol*min/ml)

TI_AUC_Drug: (=AUCtumor_Drug/AUCblood_Drug) therapeutic index for active drug

CI_Drug: (=Ctot_Drug,tumor/Cblood_Drug) concentration index for active drug

DMD Fast Forward. Published on March 20, 2008 as DOI: 10.1124/dmd.107.019182
This article has not been copyedited and formatted. The final version may differ from this version.

Appendix B: Mathematical Model and Governing Equations

The mass balance equations for the pharmacokinetic model describe the circulation of antibody-enzyme conjugate (AbE), prodrug and active drug throughout the body of a 20-gram nude mouse (Figure 1).

For large molecular weight molecules, AbE, each organ (except tumor, skin and muscle) is further divided into two subcompartments, the vascular space and extravascular space. Nnonspecific binding is not considered in those organs. A specific, saturable and reversible binding compartment is added in the extravascular space in the tumor tissue. Similarly, two endosome bound and free compartments are added as a continuation of vascular space in skin and muscle tissues. Inside all these organs or tissues, the net flux of AbE across the capillary between vascular and extravasular fluid is determined by two-pore mechanism proposed by Rippe and Haraldsson (Rippe and Haraldsson, 1987).

For small molecules, prodrug and active drug, only vascular and extravascular spaces were considered. In each subcompartment, the predisposed conjugate will convert the exiting prodrug to the active drug. In tumor tissue, both free and bound AbE will convert existing prodrug to the active drug. In skin and muscle, the predelivered endosome free and bound AbE will convert the prodrug in the vascular space to the active drug.

B.1. Mass Balance Equation for Antibody-Enzyme Conjugate (AbE)

B.1.1 Mass Balance Equation for Plasma

According to the circulation scheme illustrated, the mass balance equation for the plasma compartment is

DMD Fast Forward. Published on March 20, 2008 as DOI: 10.1124/dmd.107.019182
This article has not been copyedited and formatted. The final version may differ from this version.

$$V_{pl}(\frac{dC_{pl}}{dt} = (Q_{lung} - L_{lung})C_{v,lung} + L_{lung}C_{i,lung} + L_{liver}C_{i,liver} + L_{gi}C_{i,gi}$$
$$+ L_{spleen}C_{i,spleen} + L_{kidney}C_{i,kidney} + L_{tumor}C_{i,tumor} + L_{skin}C_{i,skin} + L_{muscle}C_{i,muscle}$$
$$+ L_{bone}C_{i,bone} + L_{heart}C_{i,heart} - (Q_{liver} + L_{gi} + L_{spleen} + Q_{kidney} + Q_{tumor} + Q_{skin}$$
$$+ Q_{muscle} + Q_{bone} + Q_{heart})C_{pl}$$

There is an additional constraint on the volumetric flow rates as

$$Q_{lung} = Q_{liver} - L_{liver} + Q_{kidney} - L_{kidney} + Q_{tumor} - L_{tumor}$$
$$+ Q_{skin} - L_{skin} + Q_{muscle} - L_{muscle} + Q_{bone} - L_{bone} + Q_{heart} - L_{heart}$$

B.1.2 Mass Balance Equation for non-eliminating organs

Vascular Space

$$J_{L,organ} = J_{iso,organ} + \alpha_L L_{organ}$$
$$J_{S,organ} = J_{iso,organ} + \alpha_S L_{organ}$$

$$V_{v,organ}(\frac{dC_{v,organ}}{dt}) = Q_{organ}C_{pl} - (Q_{organ} - L_{organ})C_{v,organ}$$
$$- J_{L,organ}(1-\sigma_L)C_{v,organ} - PS_{L,organ}(C_{v,organ} - C_{i,organ})\frac{Pe_{L,organ}}{\exp(Pe_{L,organ})-1}$$
$$- J_{S,organ}(1-\sigma_S)C_{v,organ} - PS_{S,organ}(C_{v,organ} - C_{i,organ})\frac{Pe_{S,organ}}{\exp(Pe_{S,organ})-1}$$

Interstitial Space

$$V_{i,organ}(\frac{dC_{i,organ}}{dt})$$
$$= J_{L,organ}(1-\sigma_L)C_{v,organ} + PS_{L,organ}(C_{v,organ} - C_{i,organ})\frac{Pe_{L,organ}}{\exp(Pe_{L,organ})-1}$$
$$+ J_{S,organ}(1-\sigma_S)C_{v,organ} + PS_{S,organ}(C_{v,organ} - C_{i,organ})\frac{Pe_{S,organ}}{\exp(Pe_{S,organ})-1}$$
$$- L_{organ}C_{i,organ}$$

B.1.3 Mass Balance Equation for tumor

Vascular Space

DMD Fast Forward. Published on March 20, 2008 as DOI: 10.1124/dmd.107.019182
This article has not been copyedited and formatted. The final version may differ from this version.

$$V_{v,tumor}(\frac{dC_{v,tumor}}{dt}) = Q_{tumor}C_{pl} - (Q_{tumor} - L_{tumor})C_{v,tumor}$$
$$- J_{L,tumor}(1-\sigma_L)C_{v,tumor} - PS_{L,tumor}(C_{v,tumor} - C_{i,tumor})\frac{Pe_{L,tumor}}{\exp(Pe_{L,tumor})-1}$$
$$- J_{S,tumor}(1-\sigma_S)C_{v,tumor} - PS_{S,tumor}(C_{v,tumor} - C_{i,tumor})\frac{Pe_{S,tumor}}{\exp(Pe_{S,tumor})-1}$$

Interstitial Free Concentration

$$V_{i,tumor}(\frac{dC_{if,tumor}}{dt})$$
$$= J_{L,tumor}(1-\sigma_L)C_{v,tumor} + PS_{L,tumor}(C_{v,tumor} - C_{i,tumor})\frac{Pe_{L,tumor}}{\exp(Pe_{L,tumor})-1}$$
$$+ J_{S,tumor}(1-\sigma_S)C_{v,tumor} + PS_{S,tumor}(C_{v,tumor} - C_{i,tumor})\frac{Pe_{S,tumor}}{\exp(Pe_{S,tumor})-1}$$
$$- K_{fCEA}C_{if,tumor}(B_{\max} - C_{ib,tumor})V_{i,tumor} + K_{rCEA}C_{ib,tumor}V_{i,tumor} - L_{tumor}C_{if,tumor}$$

Interstitial Bound Concentration

$$V_{i,tumor}(\frac{dC_{ib,tumor}}{dt})$$
$$= K_{fCEA}C_{if,tumor}(B_{\max} - C_{ib,tumor})V_{i,tumor} - K_{rCEA}C_{ib,tumor}V_{i,tumor}$$

B.1.4 Mass Balance Equation for skin (muscle is similar)

Vascular Space

$$V_{v,skin}(\frac{dC_{v,skin}}{dt}) = Q_{skin}C_{pl} - (Q_{skin} - L_{skin})C_{v,skin}$$
$$- J_{L,skin}(1-\sigma_L)C_{v,skin} - PS_{L,skin}(C_{v,skin} - C_{i,skin})\frac{Pe_{L,skin}}{\exp(Pe_{L,skin})-1}$$
$$- J_{S,skin}(1-\sigma_S)C_{v,skin} - PS_{S,skin}(C_{v,skin} - C_{i,skin})\frac{Pe_{S,skin}}{\exp(Pe_{S,skin})-1}$$
$$- K_{\text{int},FcRn}C_{v,skin}V_{v,skin} + K_{rec,FcRn}C_{eb,skin}V_{endo,skin}$$

The endosome is assumed to be the continuous phase of vascular space, thus the whole endosome concentration is equal to the vascular concentration for the conjugate, thus

DMD Fast Forward. Published on March 20, 2008 as DOI: 10.1124/dmd.107.019182
This article has not been copyedited and formatted. The final version may differ from this version.

$$C_{tot,endo,skin} = C_{v,skin} = \frac{A_{ef,skin} + A_{eb,skin}}{V_{endo,skin}}$$

$$V_{endo,skin} = \frac{A_{ef,skin} + A_{eb,skin}}{C_{v,skin}}$$

Interstitial Free Concentration

$$V_{i,skin}(\frac{dC_{i,skin}}{dt})$$
$$= J_{L,skin}(1-\sigma_L)C_{v,skin} + PS_{L,skin}(C_{v,skin} - C_{i,skin})\frac{Pe_{L,skin}}{\exp(Pe_{L,skin})-1}$$
$$+ J_{S,skin}(1-\sigma_S)C_{v,skin} + PS_{S,skin}(C_{v,skin} - C_{i,skin})\frac{Pe_{S,skin}}{\exp(Pe_{S,skin})-1}$$
$$- L_{skin}C_{i,skin}$$

Endosome Free Concentration

$$V_{endo,skin}(\frac{dC_{ef,skin}}{dt}) = K_{\text{int},FcRn}C_{v,skin}V_{v,skin} - K_{\deg,FcRn}C_{ef,skin}V_{endo,skin}$$
$$- K_{on,FcRn}(FcRn_{tot} - C_{eb,skin})C_{ef,skin}V_{endo,skin} + K_{off,FcRn}C_{eb,skin}V_{endo,skin}$$

Endosome Bound Concentration

$$V_{endo,skin}(\frac{dC_{eb,skin}}{dt}) =$$
$$K_{on,FcRn}(FcRn_{tot} - C_{eb,skin})C_{ef,skin}V_{endo,skin} - K_{off,FcRn}C_{eb,skin}V_{endo,skin} - K_{rec,FcRn}C_{eb,skin}V_{endo,skin}$$

B.1.2 Mass Balance Equation for liver

Vascular Space

$$V_{v,liver}(\frac{dC_{v,liver}}{dt}) = Q_{liver}C_{pl} - (Q_{liver} - L_{liver})C_{v,liver}$$
$$- J_{L,liver}(1-\sigma_L)C_{v,liver} - PS_{L,liver}(C_{v,liver} - C_{i,liver})\frac{Pe_{L,liver}}{\exp(Pe_{L,liver})-1}$$
$$- J_{S,liver}(1-\sigma_S)C_{v,liver} - PS_{S,liver}(C_{v,liver} - C_{i,liver})\frac{Pe_{S,liver}}{\exp(Pe_{S,liver})-1}$$
$$- CL_{\deg Liver}C_{v,liver}$$

DMD Fast Forward. Published on March 20, 2008 as DOI: 10.1124/dmd.107.019182
This article has not been copyedited and formatted. The final version may differ from this version.

Interstitial Space

$$V_{i,organ}(\frac{dC_{i,organ}}{dt})$$
$$= J_{L,organ}(1-\sigma_L)C_{v,organ} + PS_{L,organ}(C_{v,organ} - C_{i,organ})\frac{Pe_{L,organ}}{\exp(Pe_{L,organ})-1}$$
$$+ J_{S,organ}(1-\sigma_S)C_{v,organ} + PS_{S,organ}(C_{v,organ} - C_{i,organ})\frac{Pe_{S,organ}}{\exp(Pe_{S,organ})-1}$$
$$- L_{organ}C_{i,organ}$$

In each organ, the total (or average) concentration is the weighted average of the concentrations within each subcompartment

$$C_{tot} = \frac{C_{v,organ}V_{v,organ} + (C_{if,organ} + C_{ib,organ})V_{i,organ}}{V_{organ}}$$

Or for skin and muscle

$$C_{tot} = \frac{C_{v,organ}V_{v,organ} + C_{i,organ}V_{i,organ} + (C_{eb,organ} + C_{ef,organ})V_{endo,organ}}{V_{organ}}$$

B.2. Mass Balance Equation for Prodrug and active drug

Diffusion-limited model is assumed for both prodrug and active drug. Liver is considered as the only eliminating organ.

Prodrug in Vascular Space

$$V_{v,organ}(\frac{dC_{v\_prodrug,organ}}{dt}) = Q_{organ}(C_{pl\_prodrug} - C_{v\_prodrug,organ})$$
$$- PS_{prodrug}f_{up,prodrug}(C_{v\_prodrug,organ} - \frac{C_{i\_prodrug,organ}}{R_{prodrug,organ}})$$
$$- \frac{E_{\max,prodrug}C_{v,organ}V_{v,organ}f_{up,prodrug}C_{v\_prodrug,organ}}{EC_{50\,prodrug} + f_{up,prodrug} * C_{v\_prodrug,organ}}$$

Active Drug in Vascular Space

DMD Fast Forward. Published on March 20, 2008 as DOI: 10.1124/dmd.107.019182
This article has not been copyedited and formatted. The final version may differ from this version.

$$V_{v,organ}(\frac{dC_{v\_drug,organ}}{dt}) = Q_{organ}(C_{pl\_drug} - C_{v\_drug,organ}) - PS_{drug} f_{up,drug}(C_{v\_drug,organ} - \frac{C_{i\_drug,organ}}{R_{drug,organ}})$$
$$+ \frac{E_{\max,prodrug} C_{v,organ} V_{v,organ} f_{up,prodrug} C_{v\_prodrug,organ}}{EC_{50\,prodrug} + f_{up,prodrug} * C_{v\_prodrug,organ}}$$

Prodrug in the interstitial space

$$V_{i,organ}(\frac{dC_{i\_prodrug,organ}}{dt}) = PS_{prodrug} f_{up,prodrug}(C_{v\_prodrug,organ} - \frac{C_{i\_prodrug,organ}}{R_{prodrug,organ}})$$
$$- \frac{E_{\max,prodrug} C_{i,organ} V_{i,organ} f_{up,prodrug}(\frac{C_{i\_prodrug,organ}}{R_{prodrug,organ}})}{EC_{50\,prodrug} + f_{up,prodrug} * (\frac{C_{i\_prodrug,organ}}{R_{prodrug,organ}})}$$

Active Drug in the interstitial space

$$V_{i,organ}(\frac{dC_{i\_drug,organ}}{dt}) = PS_{drug} f_{up,drug}(C_{v\_drug,organ} - \frac{C_{i\_drug,organ}}{R_{drug,organ}})$$
$$+ \frac{E_{\max,prodrug} C_{i,organ} V_{i,organ} f_{up,prodrug}(\frac{C_{i\_prodrug,organ}}{R_{prodrug,organ}})}{EC_{50\,prodrug} + f_{up,prodrug} * (\frac{C_{i\_prodrug,organ}}{R_{prodrug,organ}})}$$